

Fall 12-2017

Computational Investigation of the Biomechanics of Babywearing in Regards to Developmental Dysplasia of the Hip

Gaurav Girish
Embry-Riddle Aeronautical University

Follow this and additional works at: <https://commons.erau.edu/edt>



Part of the [Mechanical Engineering Commons](#), and the [Other Medicine and Health Sciences Commons](#)

Scholarly Commons Citation

Girish, Gaurav, "Computational Investigation of the Biomechanics of Babywearing in Regards to Developmental Dysplasia of the Hip" (2017). *Doctoral Dissertations and Master's Theses*. 365.
<https://commons.erau.edu/edt/365>

This Thesis - Open Access is brought to you for free and open access by Scholarly Commons. It has been accepted for inclusion in Doctoral Dissertations and Master's Theses by an authorized administrator of Scholarly Commons. For more information, please contact commons@erau.edu.

COMPUTATIONAL INVESTIGATION OF THE BIOMECHANICS OF
BABYWEARING IN REGARDS TO DEVELOPMENTAL DYSPLASIA OF
THE HIP

by

Gaurav Girish

A Thesis Submitted to the College of Engineering Department of Mechanical
Engineering in Partial Fulfillment of the Requirements for the Degree of
Master of Science in Mechanical Engineering

Embry-Riddle Aeronautical University
Daytona Beach, Florida
December 2017

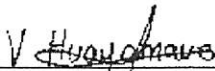
COMPUTATIONAL INVESTIGATION OF THE BIOMECHANICS OF
BABYWEARING IN REGARDS TO DEVELOPMENTAL DYSPLASIA OF
THE HIP

by

Gaurav Girish

This thesis was prepared under the direction of the candidate's Thesis Committee Chair, Dr. Victor Huayamave, Professor, Daytona Beach Campus, and Thesis Committee Members Dr. Eduardo Divo, Professor, Daytona Beach Campus, and Dr. Jean-Michel Dhainaut, Professor, Daytona Beach Campus, and has been approved by the Thesis Committee. It was submitted to the Department of Mechanical Engineering in partial fulfillment of the requirements for the degree of Master of Science in Mechanical Engineering


Thesis Review Committee:



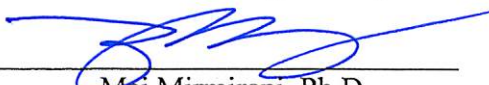
Victor Huayamave, Ph.D.
Committee Chair




Eduardo Divo, Ph.D.
Committee Member



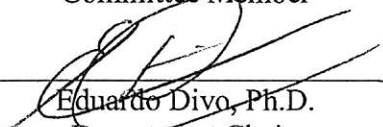
Jean-Michel Dhainaut, Ph.D.
MSME Program Coordinator,
Mechanical Engineering



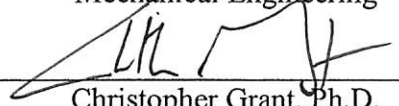
Maj Mirmirani, Ph.D.
Dean, College of Engineering



Jean-Michel Dhainaut, Ph.D.
Committee Member



Eduardo Divo, Ph.D.
Department Chair,
Mechanical Engineering



Christopher Grant, Ph.D.
Vice Chancellor of Academic Support

12/2/17
Date

Acknowledgements

I would like to thank Dr. Victor Huayamave for providing timely and constructive advice during my thesis journey. Without your guidance and insight, it would have been exceedingly difficult to continue and develop this research into the living work that it is. I would also like to thank Dr. Eduardo Divo, for without the opportunities presented by you, my passion for orthopedics and bioengineering would not have been ignited. I would like to thank Dr. Chad Price for his insight into orthopedics and his profound knowledge in pediatrics and hip dysplasia; his assistance proved invaluable in understanding the medical contexts and broader impact in the research. I would also like to thank my committee member Dr. Jean-Michel Dhainaut for his feedback during my research. I would like to thank my uncle Dr. Nandkishore Raghuram for his pediatric insight and support during my research, and I would like to thank my Mother and Father for their interest in learning what I do and support to do it. Lastly, I would like to thank also Jenn Aguinaldo and Eli Longbottom for getting me a fidget spinner and teaching me the way of spinning, so that my focus would not stray during my thesis period.

Abstract

Researcher: Gaurav Girish

Title: Computational Investigation of the Biomechanics of Babywearing in regards to Developmental Dysplasia of the Hip

Institution: Embry-Riddle Aeronautical University

Degree: Master of Science in Mechanical Engineering

Year: 2017

Developmental Dysplasia of the Hip (DDH) is a congenital condition where an infant's hip socket is either loose or otherwise unstable. DDH causes a joint instability where the femoral head is not properly situated inside the acetabulum. Etiology of the condition is in part congenital and developmental, with a difference of DDH prevalence between ethnicities. Incidence of DDH is also in some part dependent on cultural practices and activities of the mother and child. . The exact nature of this cultural incidence is not clearly understood. A computational approach is hypothesized to identify the impact of babywearing position on the healthy development of the hip at infancy. Detailed analysis of muscle force contribution and joint reaction force across the range of motion that babywearing allows can give better understanding on correct and incorrect methods of babywearing. The joint kinematics was varied across its range of motion, and the resultant joint reaction forces were analyzed. The reaction force magnitudes and directions supported the assertions of conventional wisdom in babywearing manufacture, and the M position of babywearing and any position similar to it using high hip flexions with wide abductions were found to be most conducive to healthy hip development.

Table of Contents

	Page
Thesis Review Committee	ii
Acknowledgements.....	ii
Abstract	iii
List of Tables	vi
List of Figures	vii
Chapter	
I Introduction.....	1
Anatomical Background	2
Osteoarthritis.....	3
II Review of the Relevant Literature	5
Developmental Dysplasia of the Hip	5
Treatment of DDH	7
Disease Risk Factors	10
Babywearing	11
Cultural and Ethnic Influence	13
Computational Analysis.....	17
Broader Impact.....	18
Hypothesis.....	19
III Methods.....	20
Introduction.....	20
Problem Definition.....	20

	OpenSim Model Implementation.....	21
	Thelen Muscle Model	22
	Assumptions.....	25
	Model Scaling.....	28
	Muscle Tuning	28
	Experimental Method.....	32
	Inverse Dynamics and Joint Reaction Force.....	32
IV	Results.....	35
V	Discussion.....	46
	Comparison with Existing Babywearing Positions.....	47
VI	Conclusion	51
	Future Work	51
Appendices		
A	Bibliography	53
B	Joint Reaction Force Table	55
C	Example OpenSim Files	57

List of Tables

	Page
Table	
1 JRF variation with respect to abduction on the rows and flexion on columns	38
2 Angular deviation in degrees of JRF with respect to value found from 120 flexion and 60 abduction taken using law of cosines, with 180 degrees indicating fully reversed direction of the JRF	38
3 Normalized colormap indicating percent difference of the dataset with respect to the JRF magnitude value found from 60 abduction and 120 flexion, with green indicating closest to healthy	49
4 Normalized colormap indicating percent difference of the dataset with respect to the JRF vector direction found from 60 abduction and 120 flexion, with green indicating closest to healthy	50

List of Figures

	Page
Figure	
1 Radiographic image of a healthy hip anatomy	3
2 Osteoarthritis-induced malformations on the hip socket region.....	4
3 The grades of severity of DDH, starting from Type 1 minor luxation to Type 3 full dislocation.	6
4 The Pavlik harness and short leg spica cast.....	9
5 Experimental growth measurements of the femoral head and acetabulum.	11
6 Images showing various types of babywearing methods used around the world. .	13
7 Image of a swaddled eskimo infant on a babyboard.....	14
8 Image of a Nigerian woman and two Chinese women	15
9 Cultural practice compared to the prevalence of DDH with time	16
10 Graph of DDH incidence rates between ethnicities	17
11 Visual output from research by Giorgi showing femoral head and acetabulum development when subjected to concentric and asymmetric forces in the hip joint	18
12 GUI of OpenSim and the Gait 2354 model	22
13 A representation of the hill muscle model from which the thelen model derives from and its characteristic curves	24
14 Graphic of the simplified human body model used for analysis	26
15 The Lower body joints and their directions of motion	27
16 Model muscle total force and stretch with respect to hip abduction.....	30
17 Model muscle total force and stretch with respect to hip flexion.....	31

18	A visual model of the joint reaction force tool action in OpenSim, utilizing static equilibrium of the muscle elements to determine the joint reaction forces on the bone.....	33
19	Surface Plot of the JRF with respect to flexion and abduction.....	35
20	JRF magnitude for fixed angles of abduction with respect to flexion	36
21	X-Component Force for fixed angles of abduction with respect to flexion	37
22	Y-Component Force for fixed angles of abduction with respect to flexion	37
23	Z-Component Force for fixed angles of abduction with respect to flexion.....	38
24	JRF magnitude and direction for 15 degrees of adduction and flexion varied on the axis	39
25	JRF magnitude and direction for 0 degrees of abduction with flexion varied on the axis	40
26	JRF magnitude and direction for 15 degrees of abduction with flexion varied on the axis	41
27	JRF magnitude and direction for 30 degrees of abduction with flexion varied on the axis	42
28	JRF magnitude and direction for 45 degrees of abduction with flexion varied on the axis	43
29	JRF magnitude and direction for 60 degrees of abduction with flexion varied on the axis	44
30	JRF magnitude and direction for 75 degrees of abduction with flexion varied on the axis	45
31	A visual of the babywearing styles most commonly recommended for healthy hip development, the M shape involves the baby pushed close to the chest, and the J shape involves the baby pushed close to the side of the carrier’s body.....	49

Chapter I

Introduction

Orthopedics is a fascinating science with many diverse sub-disciplines, combining medicine and engineering to solve complex problems regarding the musculoskeletal system. The science began initially as a method to repair spinal deformities in children, which is referenced in its etymology; the word orthopedics is derived from the greek words *orthos*, meaning straight, and *paidion*, meaning child [1]. The practice expanded beyond children into treatment of adult patients around the turn of the 20th century. This, along with the improvement of medicine, allowed for the expansion of the science into all things musculoskeletal. The start of more modern medical practices expanded the scope of medicine beyond retrospective treatment into preventive medicine, with computer simulations providing key insight and solutions into many musculoskeletal disorders. This thesis discusses a computational approach to preventatively treat developmental dysplasia of the hip (DDH). Large-scale patient examination has indicated a direct correlation between the incidence of DDH and the culturally preferred method of baby carrying [2]; however, the biomechanics of the baby carrying are not well understood and results are purely qualitative in nature [3]. Studies conducted utilizing a computational approach on infant bone mechanobiology have allowed for more comprehensive understanding into the factors affecting hip morphology and its consequence on DDH [4].

Anatomical Background

The hip is a complex joint comprised of many muscle and soft tissue components, connected to two main bones: The pelvis and femur. The hip region is supplied with blood from the abdominal aorta, and the joint region supplied with the iliac arteries. The joint surfaces are mostly covered in articular cartilage that allow for complete movement within the socket. The cartilage covers the pelvic acetabulum socket in a moon-shaped pattern called the lunate surface, the lunate surface encircles the ligamentum teres in the socket. The teres connects the acetabulum and the femoral head ball and loosely constrains the ball-and-socket connection. The joint is also fully constrained by the acetabular labrum, a cartilaginous tissue section that covers the acetabular rim. The entire section is wrapped in a dense tissue known as the fibrous capsule. The capsule is connected to 2 circular ligaments that strengthen the structure of the capsule. The capsule prevents egregious motion of the femoral head and seals lubrication inside the hip joint. The capsule is surrounded by muscles, which articulate the leg in the flexion, abduction, and rotation planes of motion, providing 6 degrees of freedom to the lower extremity. These muscles are innervated by the femoral nerve and its branches that pervade through the leg. The hip supports the weight of the body in static and dynamic postures, such as standing and running, respectively. The hip is also the main adjuster of posture, with the pelvic tilt defining much of the orientation of the body [5].

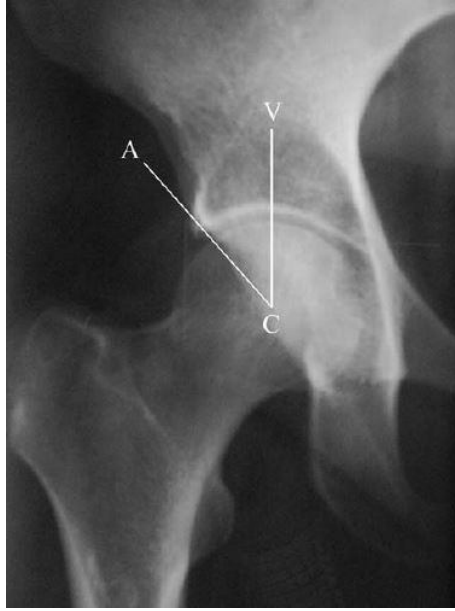


FIGURE 1.1: Radiographic image of a healthy hip anatomy [6]

Osteoarthritis

If the joint is compromised, a range of problems can occur, such as improper gait, and poor posture. Problems in the joint destabilize the biomechanical equilibrium that allows for proper bipedal movement. Unhealthy motion such as limp gait can erode tissue inside the acetabulum and femoral head connection. Such tissue erosion can produce bone on bone contact that will eventually wear away the joint itself. This type of contact has massive consequences in the way of reduced quality of life. Joint degeneration ultimately leads to hip osteoarthritis, which is a disease where the joint cartilage and bone itself break down. The symptoms of this condition include pain, stiffness, swelling, decreased range of motion, and malformations in the tissues.

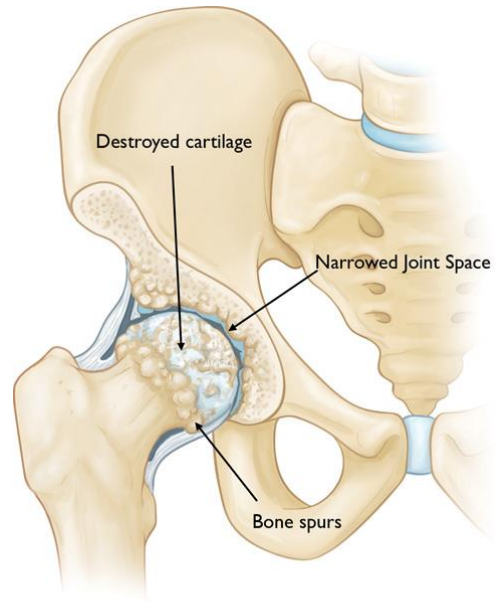


FIGURE 1.2: Osteoarthritis-induced malformations on the hip socket region [7]

Chapter II

Review of the Relevant Literature

Developmental Dysplasia of the Hip

DDH is a congenital condition where an infant's hip socket is either loose or otherwise unstable. DDH causes a joint instability where the femoral head is not properly situated inside the acetabulum [3]. Hip instability at birth is as common as 2 in 1000 live births, with the incidence being 10 times higher if the child has any family history. Females also have a higher likelihood of developing DDH due to the gender differences in pelvis morphology. Some cases of DDH spontaneously resolve, and it is unclear as to the exact mechanism of spontaneous resolution [2]. The severity of the condition can range from minute luxation, where the majority of the femoral head is still contained inside the acetabulum but is not properly situated within the socket, to large socket dislocations, which involve the head completely leaving the acetabulum and labrum. The condition can be bilateral or unilateral. Bilateral DDH is the misalignment of the left and right hip joints, whereas unilateral DDH is the instability of only a single hip socket. DDH can relate to the malformation of the acetabulum, which is called acetabular dysplasia, or the femur, which is called femoral dysplasia. Acetabular dysplasia relates to the malformation of the hip socket and the result of this malformation affecting the proper articulation of the femoral head. The usual mode of malformation for acetabular dysplasia is a socket shallowing which does not accommodate the spherical femoral head. Femoral dysplasia can involve either the distortion on the

growth of the femoral head or femoral neck. In the case of the femoral neck, if the head grows at an angle too narrow to the femur shaft, the condition is called coxa vara, the opposite case is called coxa valga, where the head grows at an angle too wide with respect to the shaft. DDH can be holistically classified into 4 types, called grades. These classifications was developed by Graf, using sonography and ultrasound techniques to identify the physiology of DDH in infants.

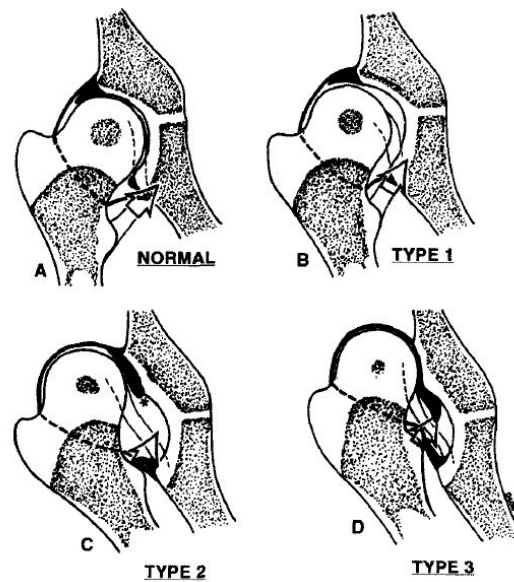


FIGURE 2.1: The grades of severity of DDH, starting from Type 1 minor luxation to Type 3 full dislocation [4]

The graf metrics of DDH are also used in conjunction with the Ortolani and Barlow tests during early infancy. The Barlow maneuver involves adducting the hip joint while applying pressure on the knee in an attempt to pop out the hip from its socket; if the hip can be popped out of socket, the maneuver results in a positive sign, and requisites the Ortolani test to confirm dislocation related to DDH. In the Ortolani test, the baby is lied down and the knees are flexed 90 degrees, the hips

are then pressured by the examiner's index fingers and abducted using the thumbs. In the case of a healthy hip, an audible "clunk" is expected. This tests for posterior dislocation and deviation from a "clunk" may indicate signs of DDH [8]. The symptoms of DDH include a discernible limp, improper gait, problems in developing proper walking technique, and an inability to walk itself. Lower grades can be asymptomatic, and external observation of the joint can be perceived as normal even past puberty into adulthood. However, the extension of tissue in more severe degrees produces muscular imbalances that weaken the overall structural integrity of the joint. The fibrous capsule weakens and stops lubricating the bone and articular cartilage. If left untreated past the period of joint ossification, DDH results in osteoarthritis and will lead to some degree of joint-replacement surgery. Surgical intervention can be prone to complication and may result in repeat procedures. Procedures are also expensive, and require post-operative care and physical rehabilitation [6]. Surgical procedure may also be required before full joint formation if the condition cannot be managed through passive measures.

Treatment of DDH

DDH can be treated through a method of surgical or nonsurgical procedures. The first line of treatment is normally nonsurgical treatment. In the case of nonsurgical, a harness, known as the Pavlik harness, is put on the child and kept on for 6-12 weeks, depending on the age of the child. The harness is a device fitted with a set of straps that restricts the range of motion of the hip joint and maintains centrally located joint reaction forces which help grow the joint normally. The harness is

removed every 1-2 weeks to check the fit of the harness, and to make adjustments as necessary. Treatment via the pavlik harness winds down to part-time wear if the hips are developing in a healthy fashion, and the child only needs to wear it at night. Success rates of the pavlik harness, although high, are not perfect, with up to 3% of cases with recurrent hip dysplasia. The pavlik harness also may produce slow development of the acetabulum, where the femoral head stays in the socket, but insufficient forces produce shallow sockets which eventually become unstable. The pavlik harness is also insufficient for greater degrees of dislocation, and in these cases treatment with the pavlik harness have higher rates of recurrence of hip dysplasia. If the harness fails, doctors may use the option of an abduction brace, which is used to limit the abduction of a child to a specific angle for 8-12 weeks. This period may proceed the pavlik harness treatment time, and is dependent on doctor discretion.

Another nonsurgical treatment is the spica cast, which is a whole-body cast that is put on the child with more egregious cases of DDH. The spica cast locks the infants hips to specific joint angles for 3-6 months, the cast normally follows surgical treatment, but can also be implemented as a nonsurgical option if such a case presents itself.

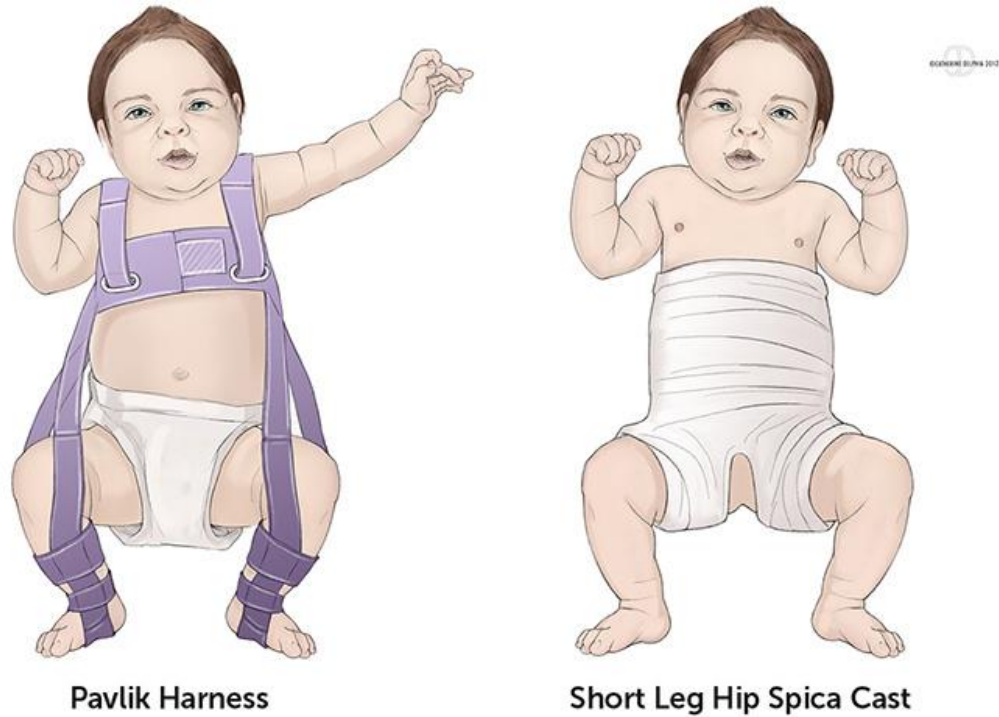


FIGURE 2.2: The Pavlik harness and short leg spica cast [14]

Surgical treatments include open and closed reduction, and either a pelvic or acetabular osteotomy. The closed reduction is a minimally invasive procedure where the doctor physically manipulates the hip joint to get the femoral head back into the acetabulum while the baby is asleep under general anesthesia. The surgery involves making an initial small incision in the groin region and surgically releasing adductor tendons, the femoral head is then manipulated back in the socket, the tendon is put back into place, and the incision is stitched up. A spica cast is then made for the child for a period of 3-6 months, and treatment transitions the cast into an abduction brace to strengthen the weakened hip muscles. Closed reduction is the most common surgical treatment for babies aged 6-24 months.

An open reduction is a procedure where surgery is required to remove and tissue that is blocking the femoral head from settling in the acetabulum, and the treatment is used for babies with more severe dislocations. The treatment has two approaches, depending on the age of the child. Both involve making a large incision near the femoral head and removing and tissue that occludes the space between the femoral head and socket. The open reduction medial approach is used when closed reductions are unsuccessful, and the anterior approach is used for older children. Anterior approach procedures may include femoral or acetabular osteotomies if the ball or socket needs to be reshaped. The postoperative path is the same as the closed reduction, and a spica cast is made for the infant, followed by an abduction brace.

Disease Risk Factors

DDH risk factors starts at fetal development. In the first and second trimesters, development progresses as normal in healthy cases; however, during later stages of pregnancy, when the bone structures are near full formation, hydrostatic forces caused by the fetal suspension in the surrounding amniotic fluid result in the structural change of the hip socket. The less force directed centrally to the acetabulum, the less concave the socket. This results in the socket becoming shallower. Shallower sockets increase the likelihood of hip instability up until birth, and is highly dependent on the random movements of the fetus. An example of such movements involve random kicking within the amniotic sac, as well as other fetal movement during pregnancy. Other factors include breech births, where

the baby is born feet-first, and the femoral head gets pushed out of the socket, and Oligohydramnios, where the lack of amniotic fluid changes the hydrostatic environment around the fetus such that the forces on the hip joint during pregnancy are not normal. Other factors that influence DDH include genetics, and whether the baby is firstborn. Bone and joint growth are directly correlated to the load that the joint holds, and development changes with respect to chronic changes in loading [9].

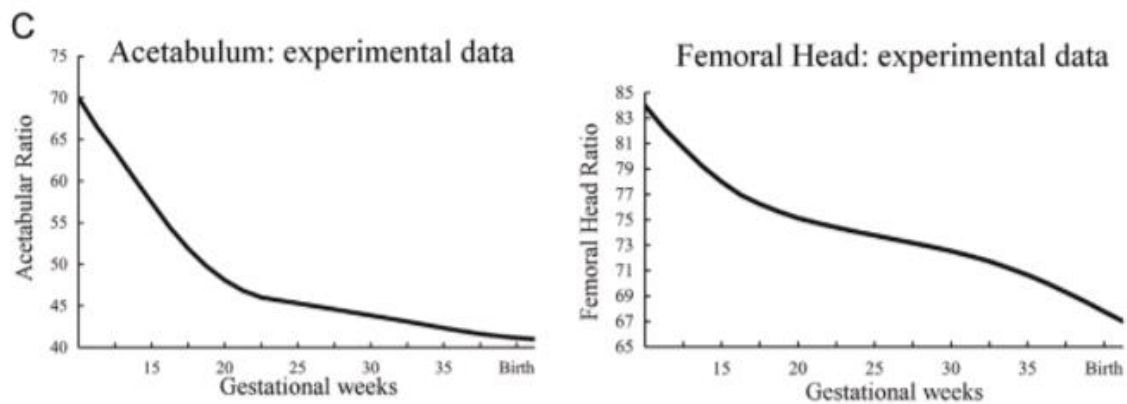


FIGURE 2.3: Experimental growth measurements of the femoral head and acetabulum [9].

Babywearing

Babywearing is the practice of carrying a baby in some form of wearer device. Babywearing has been practiced throughout history among all cultures, although the specifics in carrying practice remain unique to certain cultures. Babywearing is an effective method of carrying a child and helps improve the mental health of the mother and child, improving maternal bond. Similarly, babywearing improves paternal bond if the child is carried by the father. Babywearing also has numerous

physical health benefits for the child; it improves mental acuity, allows for faster acquisition of language, and improves bodily health. Babywearing has increased in popularity in modern times, with both swaddling and baby wrapping experiencing upticks in prevalence in different countries around the world [13].



FIGURE 2.4: Images showing various types of babywearing methods used around the world

Cultural and Ethnic Influence

Incidence of DDH is also non-uniform across ethnicities; it is in some part dependent on cultural practices and activities of the mother and child. Historically, there has been an abnormally high incidence of DDH in Eskimos that swaddle their children [10], which limits and confines the developing hips, leading to improper development.

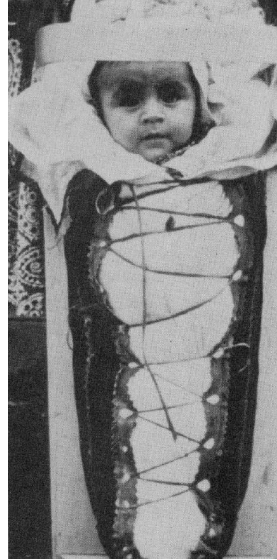


FIGURE 2.5: Image of a swaddled eskimo infant on a babyboard [2].

Conversely, Bantu peoples in eastern Africa, who practice the back-carrying method of babywearing, have an extremely low incidence of DDH [11]. The nature of this cultural incidence is based on the ubiquitous usage of specific babywearing methods. A study was conducted in Malawi examining over 40,000 children over a period of 10 years, where there was a zero-incidence of DDH being recorded. The sample size in question had mothers who almost exclusively back-carried their infants, due to the lack of availability of modern infant transport methods such as a baby stroller [3]. Other low-incidence cultures include agricultural Indian families, whose mothers carry their child on the side of their abdomen while they work in the fields during the day, and Chinese mothers, who also practice back carrying and baby-wrapping when going about their day [9].



FIGURE 2.6: Image of a Nigerian woman and two Chinese women [2]

Babywearing periods can last the entire working day, as mothers only set the baby down during cooking times and times of rest [2]. Baby wearing normally is practiced until toddlerhood, where the child starts to be able to walk under their own power and independently develop the muscles and positions required for healthy hips. As such, babywearing methods and practice are shown to be highly correlated with incidence of hip instability. DDH rates are also not constant. Due to changes in popular practice in regards to babywearing, DDH rates are rising or falling in different countries.

Chinese, Bantu, Nigerian

Rare hip dysplasia, rare hip arthritis in adults. Infants in these cultures are carried with hips abducted.

RB Salter, JBJS-Am 1966;48A:1413-39



FIG. 1. Reclining in Hong Kong Chinese. Hips are flexed and abducted.
AR Hodgson, Brit Med J 1961;2:647



Navajo Indians

Before 1940 - Cradle board without diapers: 2.7% had hip dislocations
After 1960 - diapers introduced: 0.7% had hip dislocations

DL Rabin, et al, Am J Public Health 1965;55(2):1-44



Japan

1965: 3% incidence of hip dislocation
In spite of screening
1975: National program eliminated swaddling
1984: 0.2% incidence of hip dislocation

Yamamuro, Ishida CORR 1984;184:34-40



Australia

2003: Increasing popularity of baby wrapping (Swaddling)

After 2003:
• National increase in DDH
• Increase by three fold in one region

N Williams, et al, MJA 2012;197(5):272

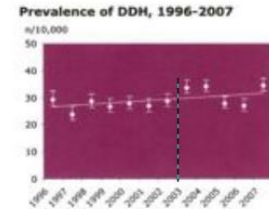


FIGURE 2.7: Cultural practice compared to the prevalence of DDH with time [12]

The cause and the nature of impact from babywearing methods in reducing DDH is not well understood. Clinical studies are limited in scope for a comprehensive understanding of the mechanism of action the baby wearing employs. Sample-based studies can only provide case-dependent and multi-factorial results, and control is too limited to concretely examine mechanical cause factors. Experiment control in *in vivo* studies for larger sample sizes cannot account for the numerous factors associated with the type and severity of each individual case of DDH, which limits result granularity and the conclusions that can be made from the existing research.

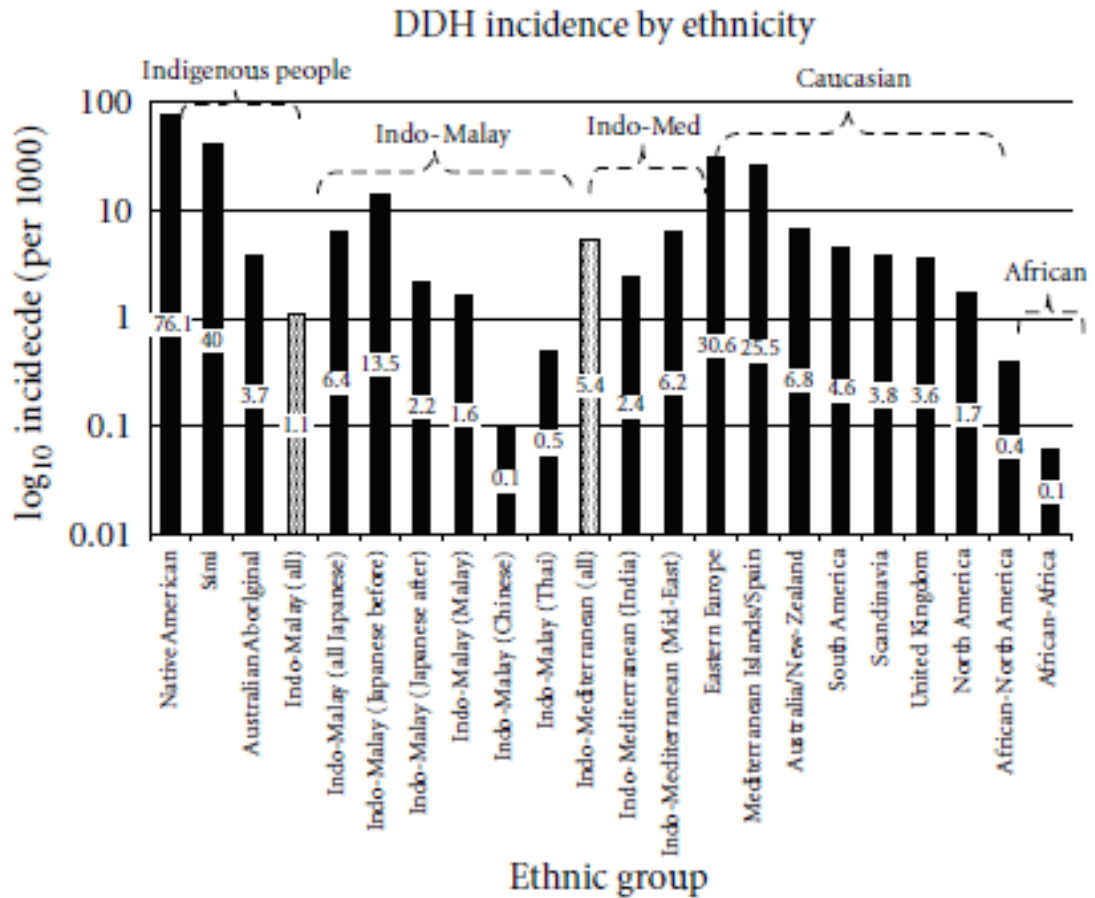


FIGURE 2.8: Graph of DDH incidence rates between ethnicities [13]

Computational Analysis

Computational investigation techniques offer many advantages compared to standard experimentation in when investigating biomechanisms. Computational methods provide detailed examinations into individual components of a biomechanical process. In this case, a computational approach allows for greater understanding of the muscle and joint reaction forces that are active of an infant while in a babywearing position. Previous research has demonstrated that joint reaction magnitude and direction is directly linked to the development of femoral

head and acetabulum structure and health [9]. Computational approaches are also more controllable than experimentation, and vacuum scenarios disregarding intrinsic factors can be more clearly defined.

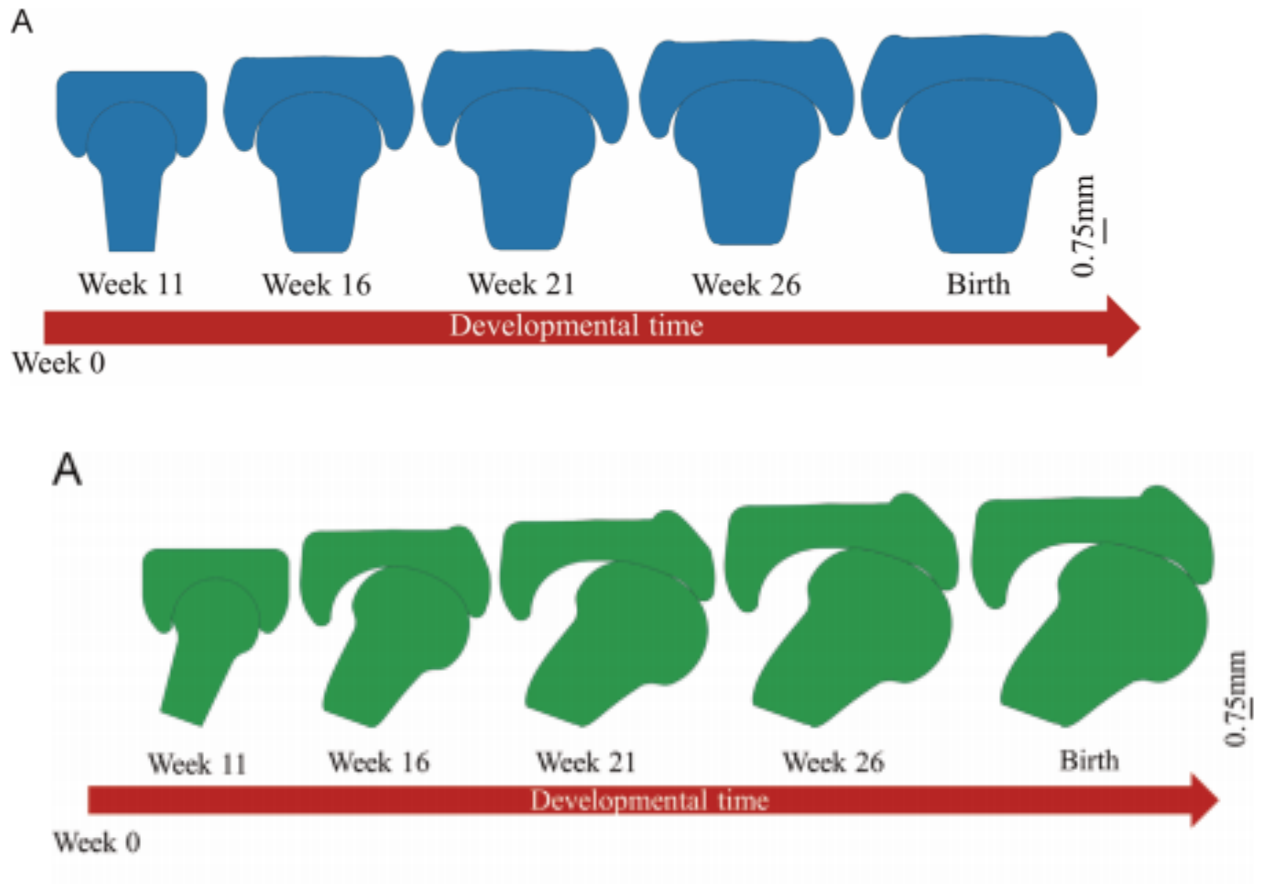


FIGURE 2.9: Visual output from research by Giorgi [9] showing femoral head and acetabulum development when subjected to concentric and asymmetric forces in the hip joint

Broader Impact

The prevention and management of DDH is of significant importance in the healthcare industry today. Osteoarthritis is one of the most common chronic conditions affecting Americans, with as many as 27 million being affected. This

study will allow for the reduction of that number with new public health initiatives being developed from the insight gained and reduce the great burden on healthcare costs for the future. Additionally, total hip replacement surgery is the most common surgery undertaken in the US [12], and has potential for postoperative complications, and the mitigation of osteoarthritis reduces the need for surgery. Any steps that are able to reduce the incidence of DDH allows for an improvement in overall public health and quality of life [3].

Hypothesis

A computational approach is hypothesized to identify the impact of babywearing position on the healthy development of the hip at infancy. Detailed analysis of muscle force contribution and joint reaction force (JRF) across the range of motion that babywearing allows a better understanding on correct and incorrect methods of babywearing. Moreover, the data obtained from this study can be used by babywearing device manufacturers to integrate and improve the products they develop.

Chapter III

Methods

Introduction

Human body movement analysis is a complex problem that requires difficulty to properly characterize the biomechanical forces in play. Numerous agonist-antagonist muscle pairs provide an indeterminate problem with many degrees of freedom that cannot be directly solved. Direct dissection of in vivo fetal hip joints is infeasible on ethical and practical grounds, and muscles and joints behave very differently under dissection. Therefore, the chosen computational method of study is position analysis, where the hip joint is varied across its range of motion to investigate the joint reaction forces returned.

Problem Definition

The problem can be defined as an inverse dynamics (ID) problem, where a desired set of kinematics data is input into a human rigid body dynamic model to get forces and moments. In the context of this analysis, the inverse dynamics problem is restricted to the hip joint, which has a set of constraints that limit the number of reactions developed. As a ball-and-socket joint, the hip resists no rotations, but prevents translations. Therefore, the only values that will be used from this analysis is the joint reaction forces in euclidean space. Before one proceeds, key assumptions are required to conduct the analysis. As previously mentioned, there is a dearth of data regarding mechanical and material properties regarding human

infants. This is rectified in the understanding that muscle behavior at the sarcomere scale is independent of geometry, and so the muscle will exhibit similar characteristic behavior in any configuration.

OpenSim Model Implementation

OpenSim is the chosen software to use for this project. The software is an open source, extensible human body modeling software initially designed for gait analysis. OpenSim has many features integrated into a pipeline paradigm that allows for the solution of inverse kinematics and inverse dynamics problems. OpenSim provides easy manipulation of human body parameters as well. In the context of this project, the joint kinematic data is an input, and the inverse dynamics problem is constrained to the hip region. The software has validated models, that were developed through a combination of MRI, CT, and dissections to identify geometries of muscles and their respective attachment points. OpenSim was also chosen due to its capabilities and ease of use when scaling these human body models. Validated models ensure biofidelity of the obtained results, and the scaling tools allow one to develop a human body model at the size and age of choice and obtain the desired mechanics. The model itself is the Gait 2354 human body model, a model developed from the Gait 2392 model by [10]. It is a 23 degree of freedom, 54 musculotendon element lower extremity model. The Gait 2354 model was chosen as it demonstrated equal solution validity to the Gait 2392 model, being directly developed from there. The Gait 2354 model also was more computationally efficient and had reduced runtimes compared to the 92

musculotendon actuator model, additionally, the 54 actuator model is easier to manipulate and tune.

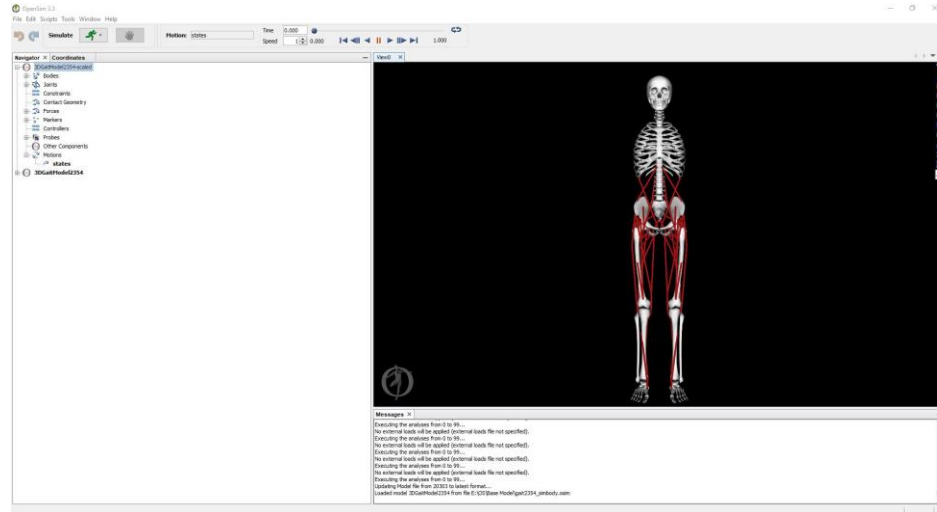


FIGURE 3.1: GUI of OpenSim and the Gait 2354 model [10]

Thelen Muscle Model

The Thelen muscle model is the model used in the Gait 2354 model. It is a Zajac-type muscle model with slight modifications based on the work of Thelen. The muscle model defines the behavior exhibited by the spring elements between the bone rigid bodies. The model defines the cable as a series of muscle and tendon elements. The muscle is modeled as a nonlinear spring with a contractile element in parallel, and the tendon is a simple elastic element. The input variables are the activation $a(t)$, a time-dependent term between 0 and 1. In this analysis the activation is assumed to be 1 and all muscles involved in the position are fully activated. The other input variable into the model is fiber length $l^M(t)$; the two input variables are input into the model to determine the stretch of muscles, which

in turn is used to develop the muscle-tendon actuator force, which is calculated via the differential equation below:

$$(1) \quad f_{iso}(a(t)f_{AL}(l_M)f_v(\dot{l}_M) + f_{PL}(l_M))\cos\alpha - f_{iso}f_{SE}(l_T) = 0$$

Where f_{iso} is the maximum isometric force, f_{AL} is the active tension portion of the muscle force, f_v is the force developed from the muscle fiber velocity, f_{PL} is the passive tension portion of the muscle force, f_{SE} is the tendon force, α is the pennation angle, and l_T is the tendon length. The model includes muscle properties and resolves geometries through shape factors and shape-force relationships. These numbers may vary between muscles, but most terms stay constant as characterized in the Gait 2354 model. The constant terms are developed based on a resting sarcomere length of $2.2\mu\text{m}$, which is taken from estimations based on sliding filament theory. Other constant terms are developed from adult muscle material properties and shape factors related to the characteristic curves. The final terms that are constant between all muscles is the default activation and the time constants related to ramping up and ramping down muscle activation. The functions to develop terms such as the tendon length, are based on empirical observation of tendon-muscle geometries; they are not based cadaveric measurements and are instead calculated using estimations developed by Delp [6].

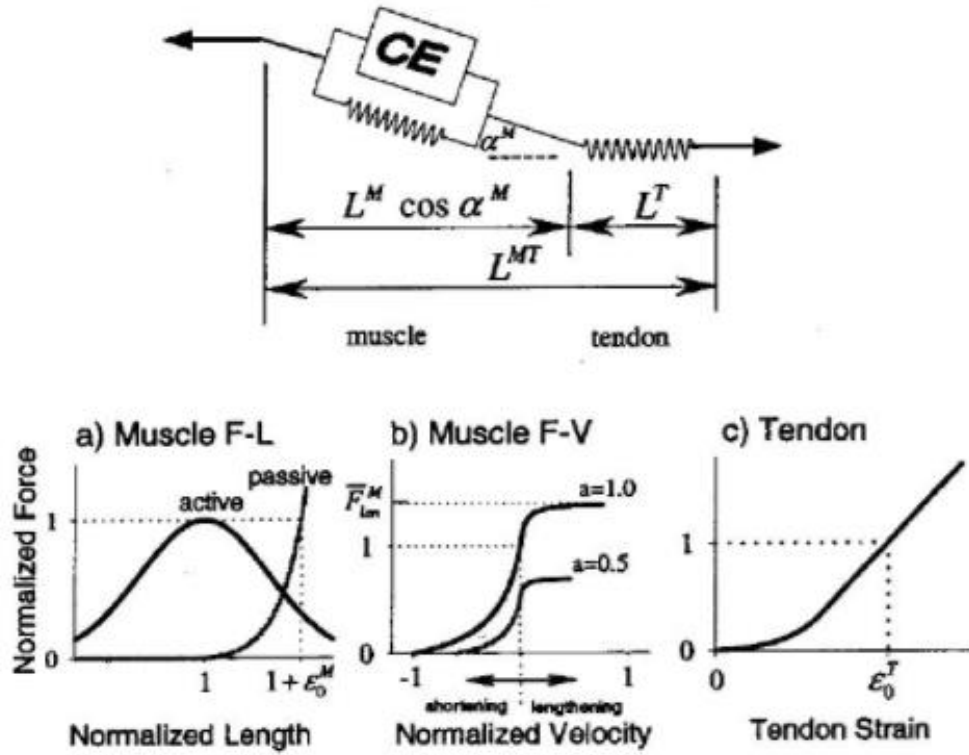


FIGURE 3.2: A representation of the hill muscle model from which the thelen model derives from and its characteristic curves [15]

The partial differential equation shown in equation 1 has four singularity conditions. They are as follows:

- (2) $a(t) \rightarrow 0$
- (3) $f_{AL}(l^M) \rightarrow 0$
- (4) $\alpha \rightarrow 90^\circ$
- (5) $f_v(l^M) \leq 0, f_v(l^M) \geq F_{len}^m$

These conditions are avoided by applying boundary conditions that limit the equation such that the solution converges. Some of these conditions are input into

the software itself or are defined by the user, depending on the analysis. The software can proceed to calculate musculotendon actuator force based on the combination of user input and preprogrammed singularity avoidance conditions, but for increased solution validity and brevity additional assumptions are involved in the analysis of this problem.

Assumptions

The primary assumption that the study uses is that all processes are quasi-static. OpenSim is primarily a gait analysis software that contains time-dependent terms that are baked into the model, with activation, a key variable, being one of the main influencers in muscle activity. However, this concern of this research is in regards to long-duration positions, in where the parent or guardian would be carrying the child for many hours at a time. It is therefore reasonable to assert that the muscles do not exhibit any time dependent behavior within the scale of the analysis. The kinematic data is adjusted to reflect this assertion, and no joint velocities or accelerations are input.

Another assumption that is used in this analysis is the simplification of muscles and tendons. OpenSim, as a rigid body dynamics software, models the muscle elements as 1 dimensional nonlinear springs. The springs behave as per the Thelen muscle model and hold active tension and passive tension, dependent on the amount of stretch. The muscle origin and insertion points are simply put into the model as positions in space. Wrapping is defined through elements pivoting around defined points, with muscles allowed to collide and intersect freely. This is not a

concern, however, as the muscles do not have any intersection problems within anatomical joint limits.

The next assumption is to simplify the musculature of the model to hone in on the chosen area of study. OpenSim has defined the model in such a way that the left and right segments behave independently from each other. This allows for the ease in reduction of the total musculotendon elements in the model. Additionally, the research is solely focused on the hip joint reaction force, so the model is further simplified to improve solution brevity. The 54 musculotendon elements is reduced to 15, which include the larger hip abductor, flexor, and external rotator muscle groups. The muscles are as follows: the Gluteus Medius and Maximus, the Biceps Femoris long and short head, the Sartorius, the Adductor Magnus, the Pectineus, the Gracilis, the Iliacus, the Psoas, and the Rectus Femoris.



FIGURE 3.3: Graphic of the simplified human body model used for analysis

Lastly, to allow for smooth scaling transition between the adult dimensions to the infant size, the muscles are assumed to have the same exact material and mechanical properties independent of age, with only physiologic cross section, maximum isometric force, and fiber length being adjusted. These terms were developed after inspection of the individual muscle actuator element properties in OpenSim. As previously discussed, many terms are constant between each muscle in the model. Additionally, the scaling tool program-controls the scaling of the tendon geometries for each muscle, which develops its tendon sizes from the lengths of each muscle.

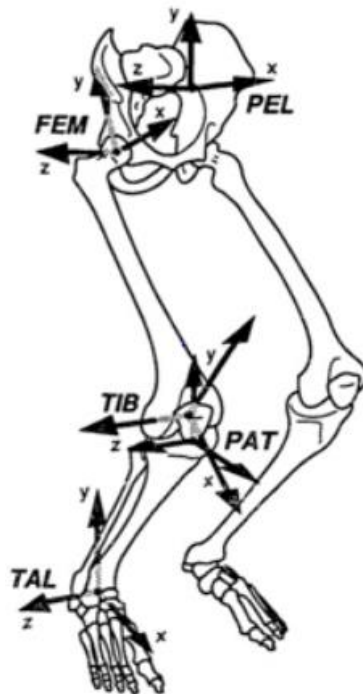


FIGURE 3.4: The Lower body joints and their directions of motion [15]

Model Scaling

With these assumptions in mind, the model is now ready to be scaled. For this research, the chosen age was 1 year. The body was scaled in accordance to the height and weight of the average 1-year old child, which was found to be 0.76 meters weighing 10.5 kg. The OpenSim Gait 2354 model initial dimensions are 1.8m weighing 76.5 N. Two scale factors were chosen to size down the adult model to infant proportions: one to reduce the overall height and one to modify the length of the femur with respect to infant proportions. The overall height scale factor that was chosen to reduce the model dimensions was 0.42, which sized down the model to an infant which would have a body surface area of 0.53 m² and a femoral length of 12 cm [16]. The next scale factor was chosen to change the size of the femur to the infant proportions, the size was taken with respect to tibial length and was found to be 0.75; this factor resolved the concern of differences between the adult proportions of the Gait 2354 model and the infant model [17].

Muscle Tuning

As the model geometry has a need to be appropriately scaled, so does the muscle forces themselves. A single scale factor is needed to modify the maximum isometric force of the muscles in the model, as OpenSim program-controls the scaling of the optimal muscle length to normalize the active-passive tension behavior. All other muscle properties need not be modified as they are independent of size. The muscle force scale factor was taken from examination of rectus femoris dimensions from infant MRIs. The length and thickness of the muscle were

recorded, with the pennation derived from literature. The terms were then calculated to find the physiologic cross-sectional area (PCSA) of the infant muscle. The muscle was then compared to the adult rectus femoris PCSA taken from [14], and a scale factor of 0.16 was developed. The scaled PCSA was then multiplied by a C value of 55.5 N/m^2 , a term used to relate the muscular isometric force with its cross-sectional area [18]. C and the maximum isometric force is related through the equation below:

$$(6) \quad f_{ISO} = C * PCSA$$

C was taken from literature and found to be independent of age [20]. With the scaling and tuning parameters, the model is appropriate for kinematic analysis to obtain infant joint reaction forces.

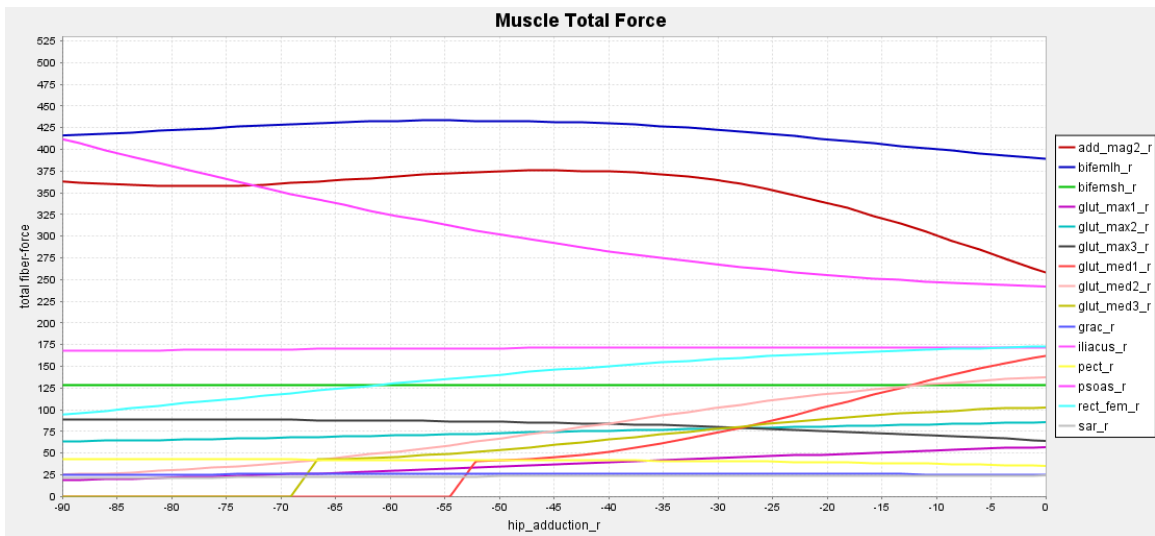
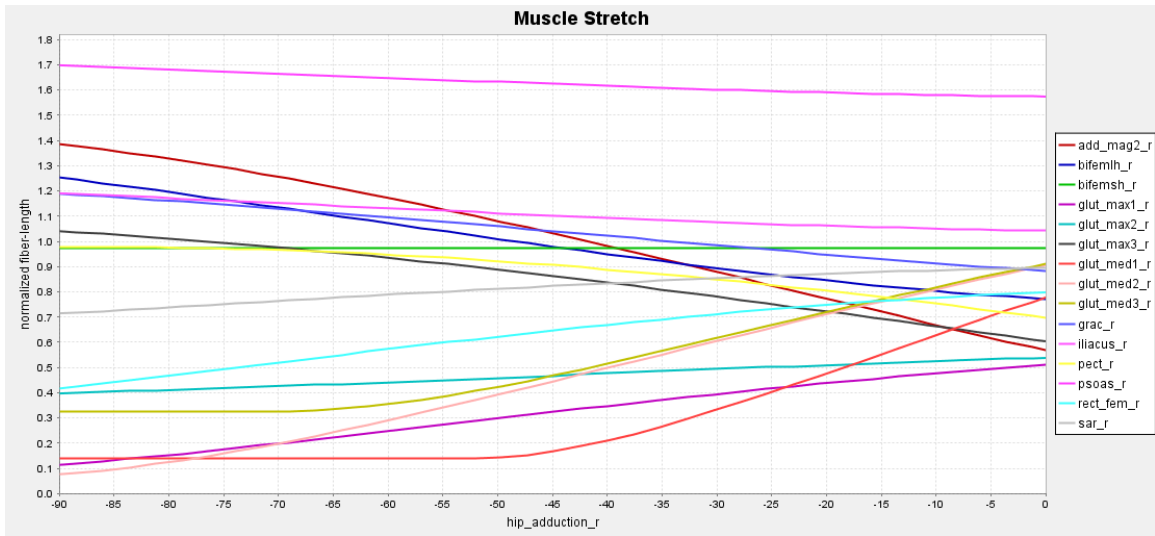


FIGURE 3.5: Model muscle total force and stretch with respect to hip abduction

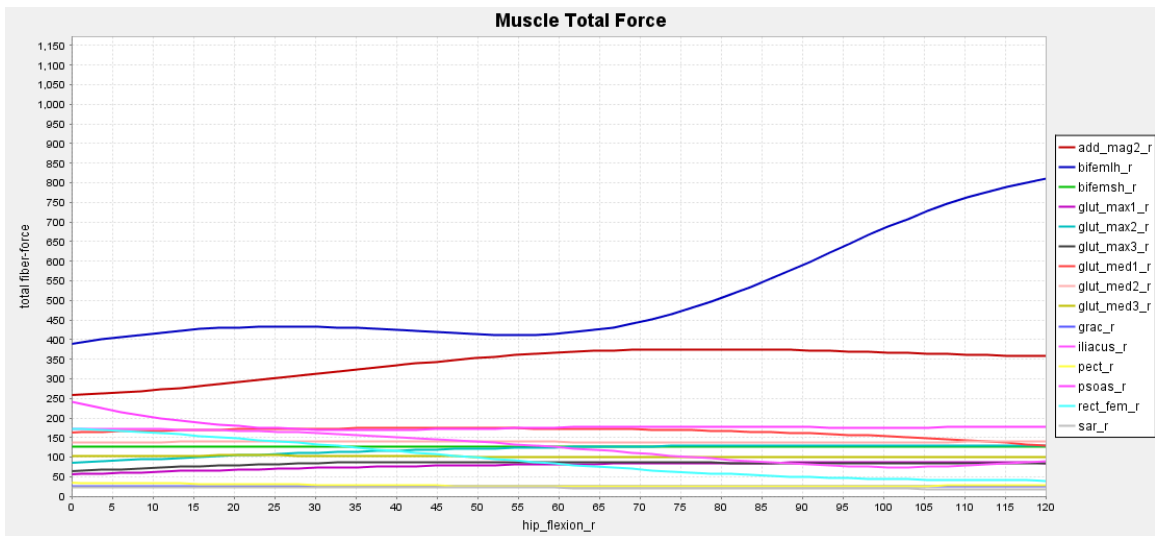
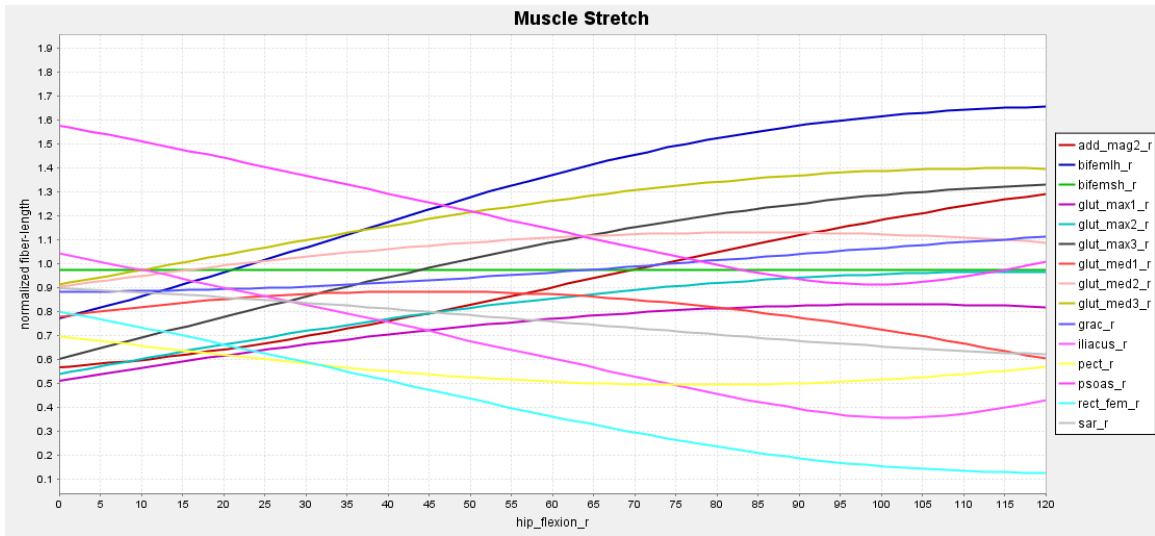


FIGURE 3.6: Model muscle total force and stretch with respect to hip flexion

Experimental Method

There is little data regarding the joint angles and kinematics utilized by babywearing device manufacturers to develop their product, so instead the joint is incremented across its range of motion in flexion and abduction to identify the development of force across the 2 axes. External rotation was fixed at 10 degrees, as many devices generally maintain the leg at this angle. The range for flexion is 0-120 degrees, and the range of abduction is -15-75 degrees, both incremented at 15 degrees. The result is 54 joint kinematic inputs points, in which the joint reaction forces be output and analyzed.

Inverse Dynamics and Joint Reaction Force

After all the inputs have been collected, the inverse dynamics analysis can begin. The inverse dynamics analysis used by OpenSim resolves the classical equations of motion to obtain the vector of generalized forces. The equation is a modification of Newton's second law and is shown below:

$$(7) \quad \sum F_{external} + \sum F_{muscles} + R_{i+1} + R_i = M_i a_i$$

Where M is the mass of the bone in analysis, and R_i and R_{i+1} are the bone reaction forces in the proximal and distal directions, respectively. The inverse dynamics algorithm in OpenSim traverses across the joints and calculates the forces and moments experienced by each joint. The joint reaction tool takes this one step further and resolves the forces and moments with respect to the joint kinematic

constraints. As previously stated, the hip is a ball and socket joint, and therefore the hip joint will resist only translational motion and rotational motion at the joint limits. In this study, the hip joint limits will not be experienced at any time, so only the joint reaction force vector will be obtained.

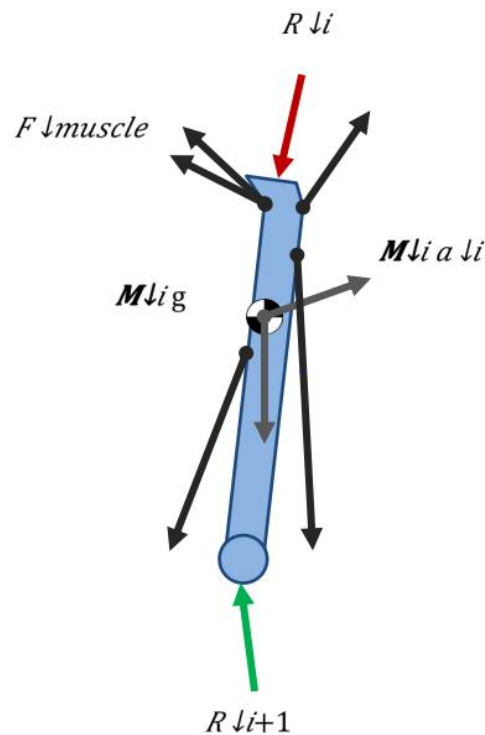


FIGURE 3.7: A visual model of the joint reaction force tool action in OpenSim, utilizing static equilibrium of the muscle elements to determine the joint reaction forces on the bone.

This study also utilizes no external forces and no motion, so the external force term and net moment term become zero. The muscles are also set to be fully activated and apply their own forces to develop the equation of equilibrium and constrain the solution. This produces an equation where the sum of the proximal

and distal reaction forces and the muscle forces equals to zero; the reactions are then calculated and output in the global reference frame, which also doubles as the pelvis reference frame. The axes originate from the center of the acetabulum.

Chapter IV

Results

This section details the resultant joint reaction force (JRF) that were developed after analyzing the input joint kinematics. The JRF output from OpenSim is a 3-dimensional vector in absolute reference frame in euclidean space. The vector originates from the geometric center of the femoral head, and the vector magnitudes were also computed. The JRFs are tabulated for the full range of motion. The average JRF magnitude across the full range of motion was 204.15 N. The smallest JRF obtained was 101.41 N, which was developed from 60 degrees of flexion and 0 degrees of abduction. The largest force is found to be 420.11 N, which was from 0 degrees of flexion and 75 degrees of abduction.

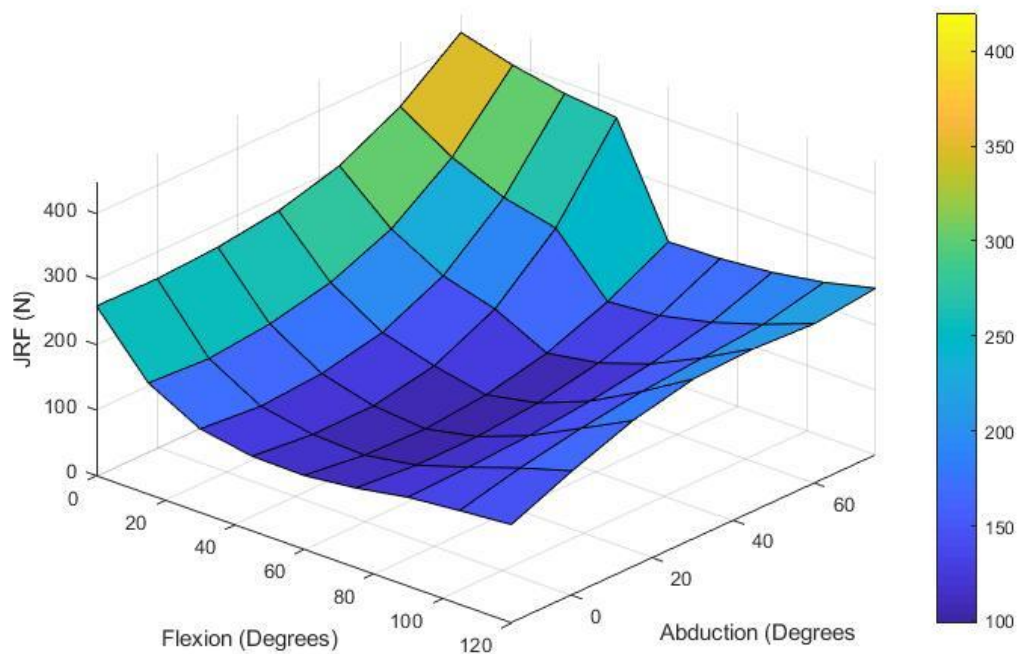


FIGURE 4.1: Surface Plot of the JRF with respect to flexion and abduction

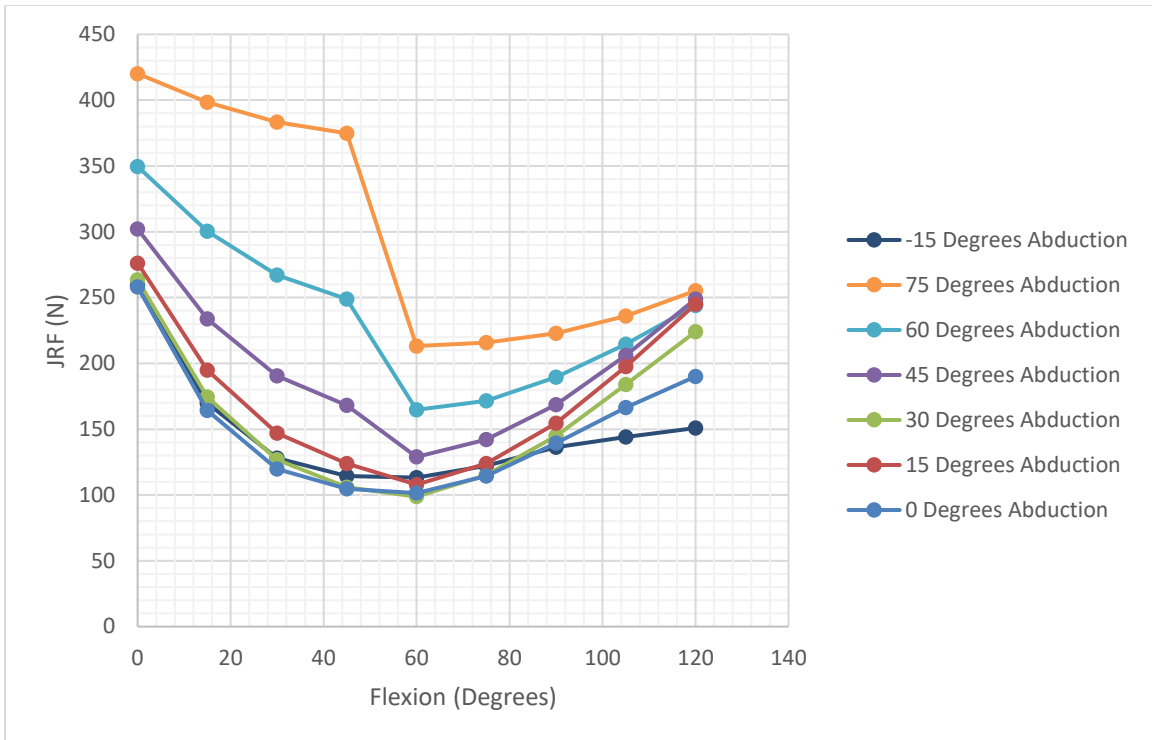


FIGURE 4.2: JRF magnitude for fixed angles of abduction with respect to flexion

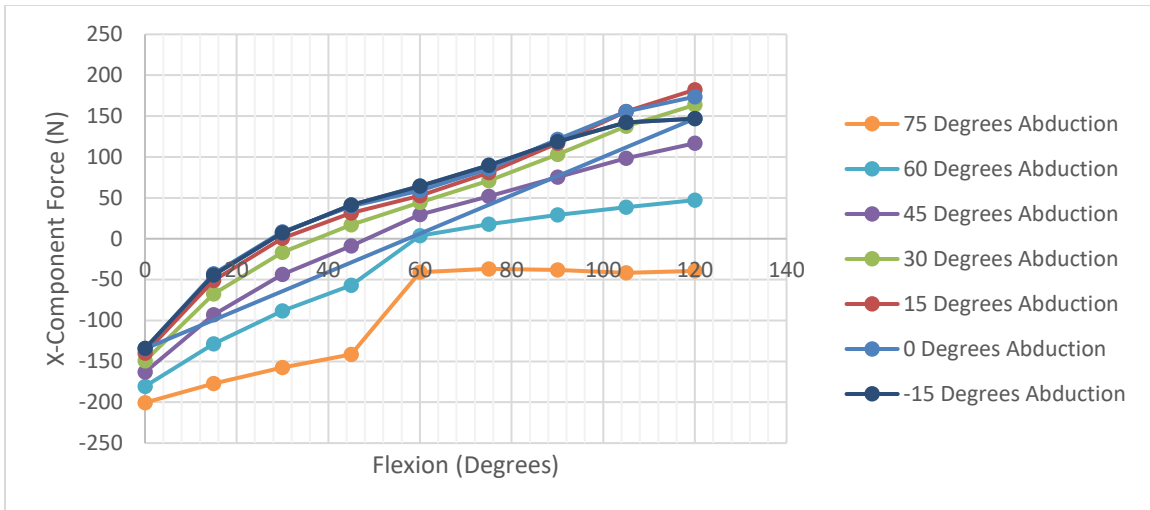


FIGURE 4.3: X-Component Force for fixed angles of abduction with respect to flexion

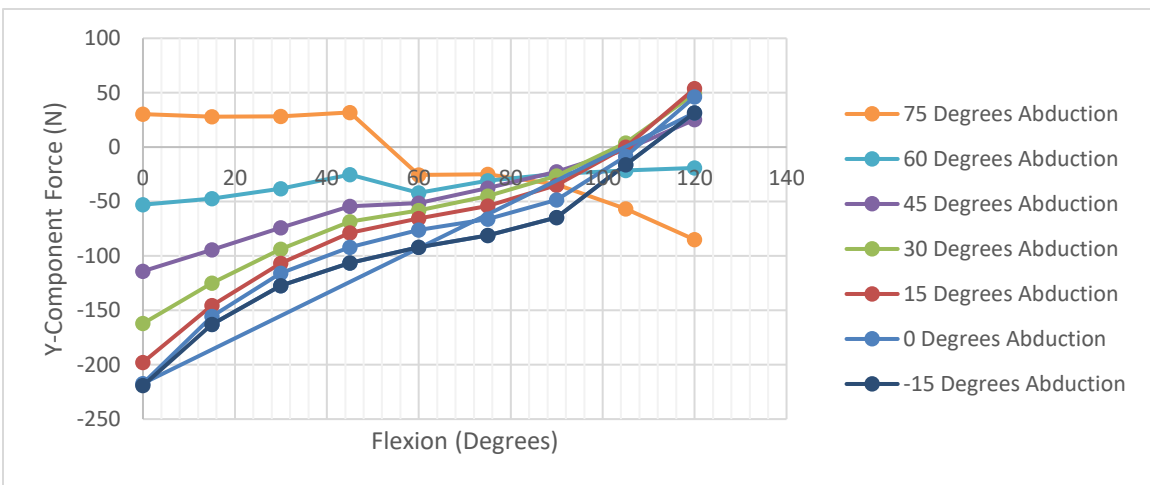


FIGURE 4.4: Y-Component Force for fixed angles of abduction with respect to flexion

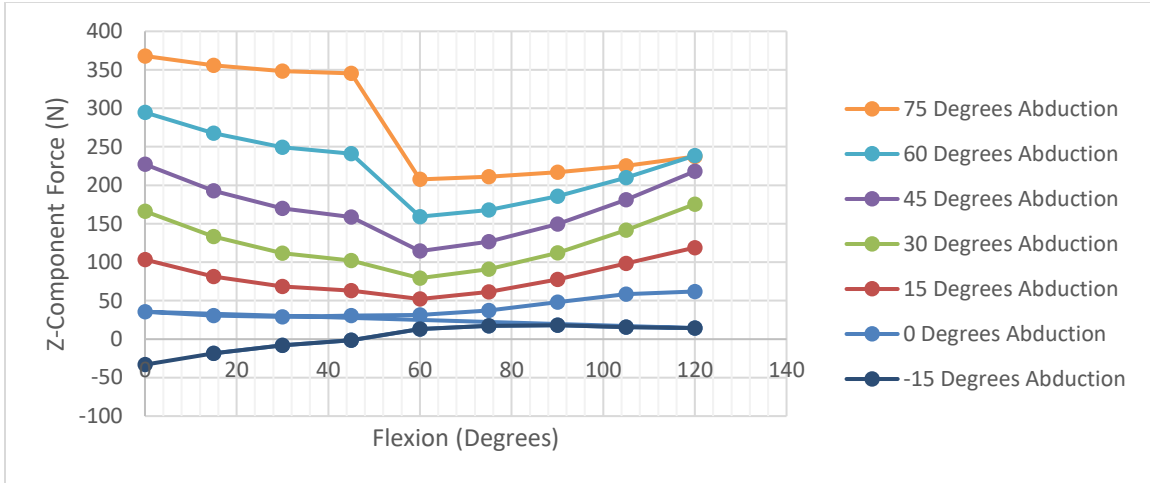


FIGURE 4.5: Z-Component Force for fixed angles of abduction with respect to flexion

TABLE 4.1: JRF variation with respect to abduction on the rows and flexion on columns

	0	15	30	45	60	75	90	105	120
-15	259.19	169.83	127.94	114.34	113.19	122.21	136.32	144.15	150.89
0	258.03	164.24	119.75	104.71	101.42	114.37	139.32	166.54	190.06
15	263.40	174.40	126.78	105.81	98.75	115.11	144.71	184.02	224.14
30	276.19	194.85	146.87	123.95	107.90	123.77	154.47	197.46	244.91
45	302.10	233.82	190.41	168.04	128.91	142.00	168.67	206.10	248.78
60	349.56	300.49	267.20	248.85	164.69	171.54	189.55	214.47	244.02
75	420.11	398.33	383.21	374.75	213.16	215.79	222.90	235.87	255.09

TABLE 4.2: Angular deviation in degrees of JRF with respect to value found from 120 flexion and 60 abduction taken using law of cosines, with 180 degrees indicating fully reversed direction of the JRF

	0	15	30	45	60	75	90	105	120
-15	99.13	94.65	88.48	82.43	73.30	70.58	70.40	72.21	74.63
0	84.21	78.17	70.99	64.69	61.65	59.35	57.70	58.13	61.55
15	70.14	62.29	53.55	45.71	47.84	45.94	45.55	46.69	48.90
30	57.98	49.28	39.43	29.07	32.79	30.95	31.57	33.36	35.50
45	48.66	40.44	30.86	20.05	19.26	15.36	15.74	17.73	19.82
60	42.60	36.85	30.69	24.46	14.13	7.73	3.70	1.48	0.00
75	40.67	38.56	36.54	34.72	22.40	21.10	21.50	23.35	25.03

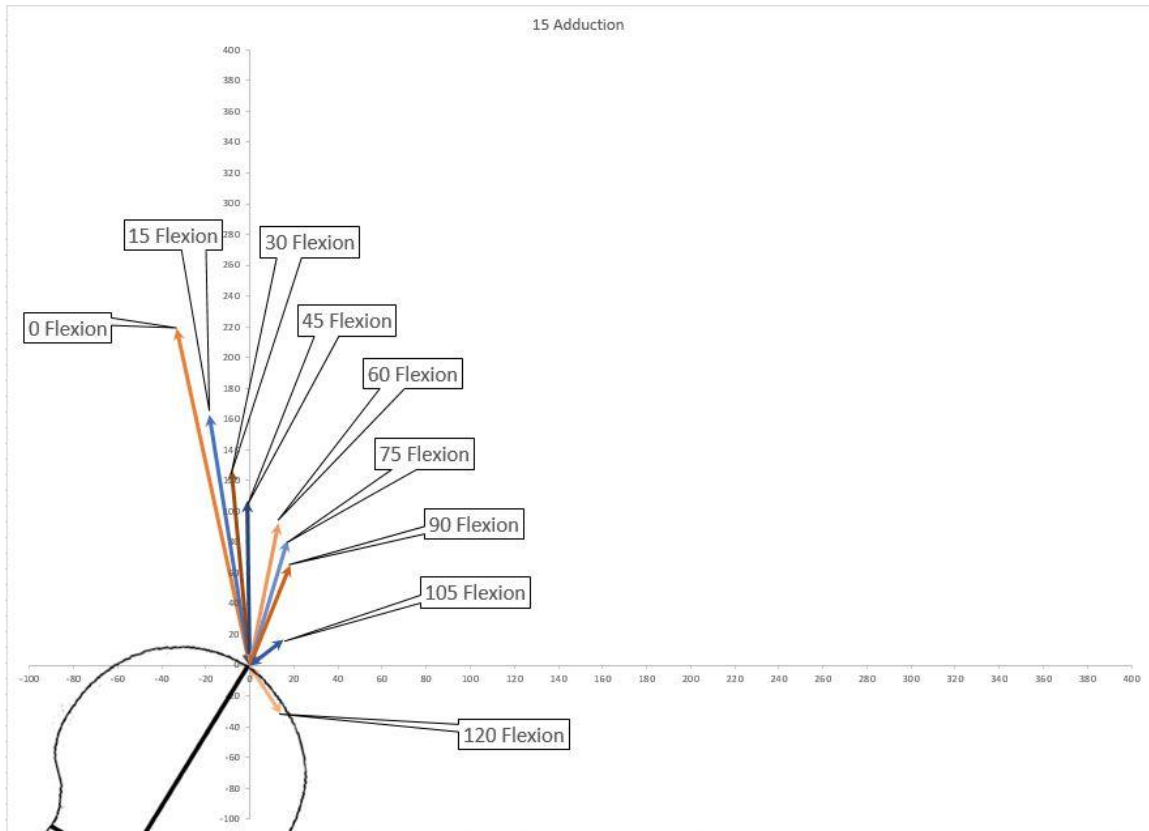


FIGURE 4.6: JRF magnitude and direction for 15 degrees of adduction and flexion varied on the axis

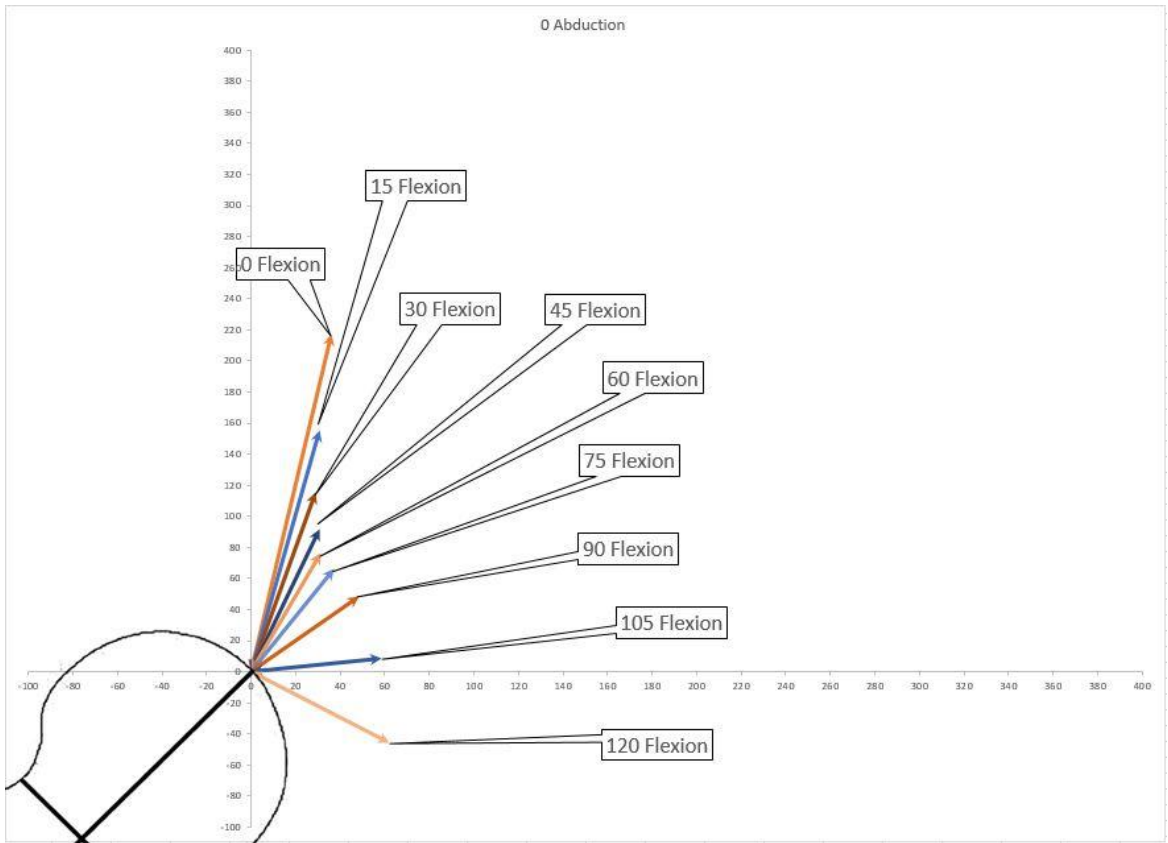


FIGURE 4.7: JRF magnitude and direction for 0 degrees of abduction with flexion varied on the axis

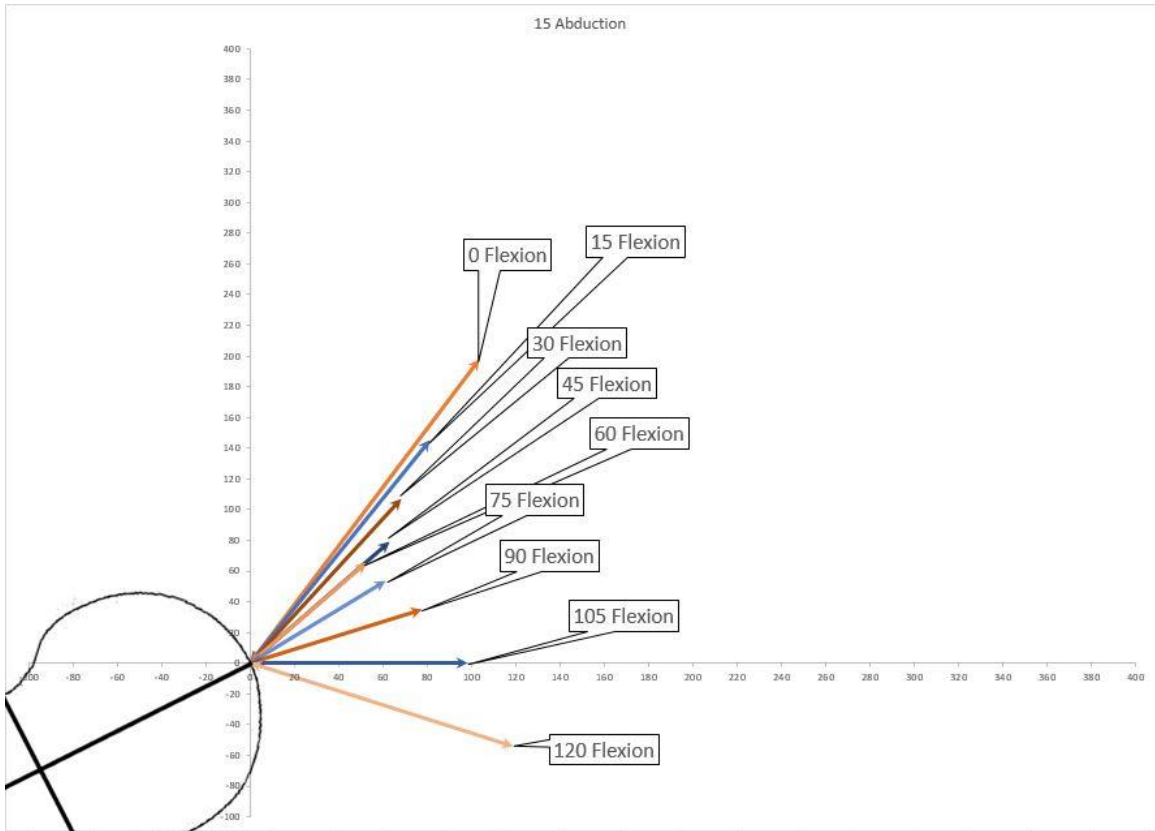


FIGURE 4.8: JRF magnitude and direction for 15 degrees of abduction with flexion varied on the axis

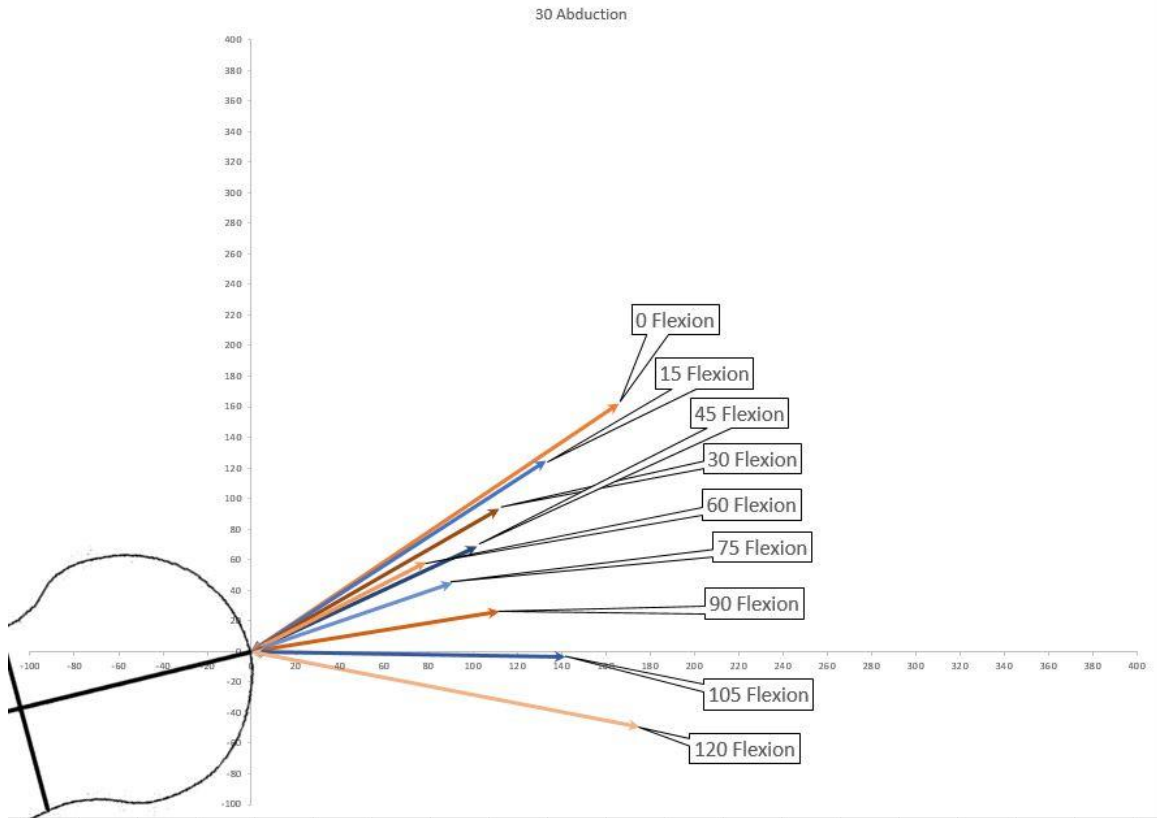


FIGURE 4.9: JRF magnitude and direction for 30 degrees of abduction with flexion varied on the axis

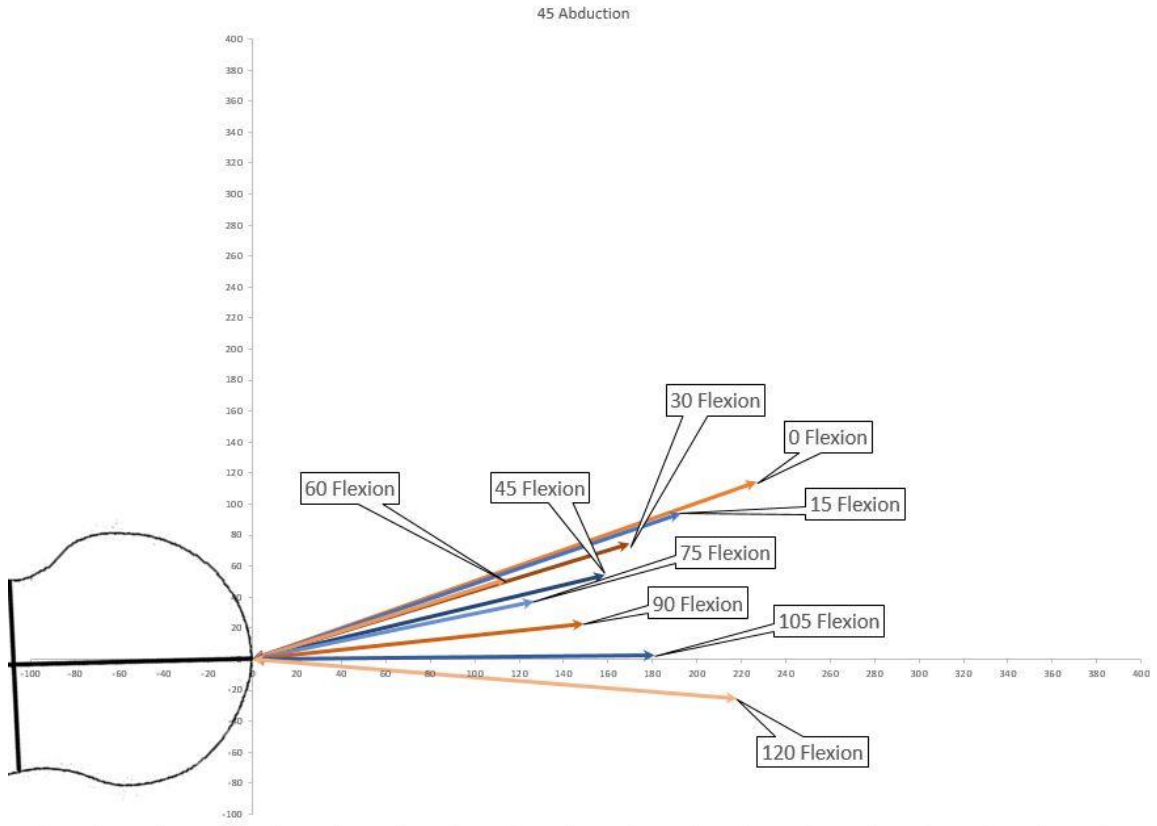


FIGURE 4.10: JRF magnitude and direction for 45 degrees of abduction with flexion varied on the axis

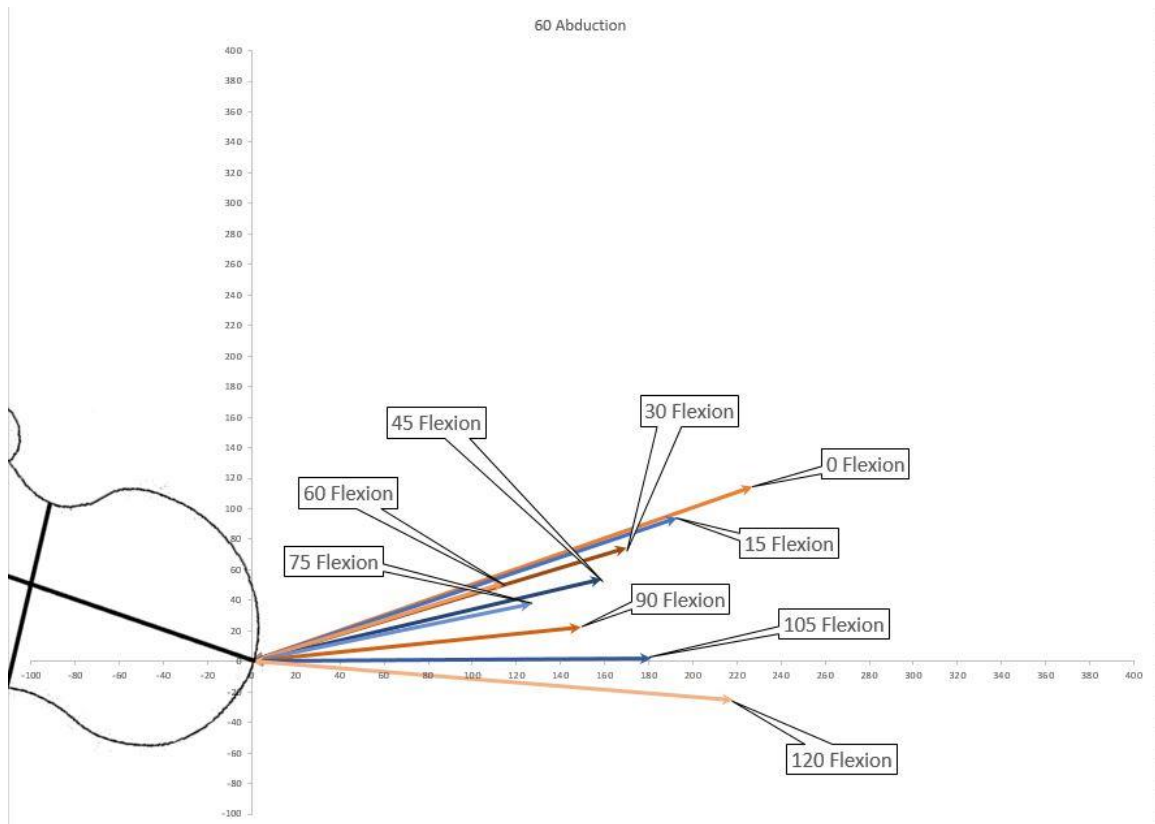


FIGURE 4.11: JRF magnitude and direction for 60 degrees of abduction with flexion varied on the axis

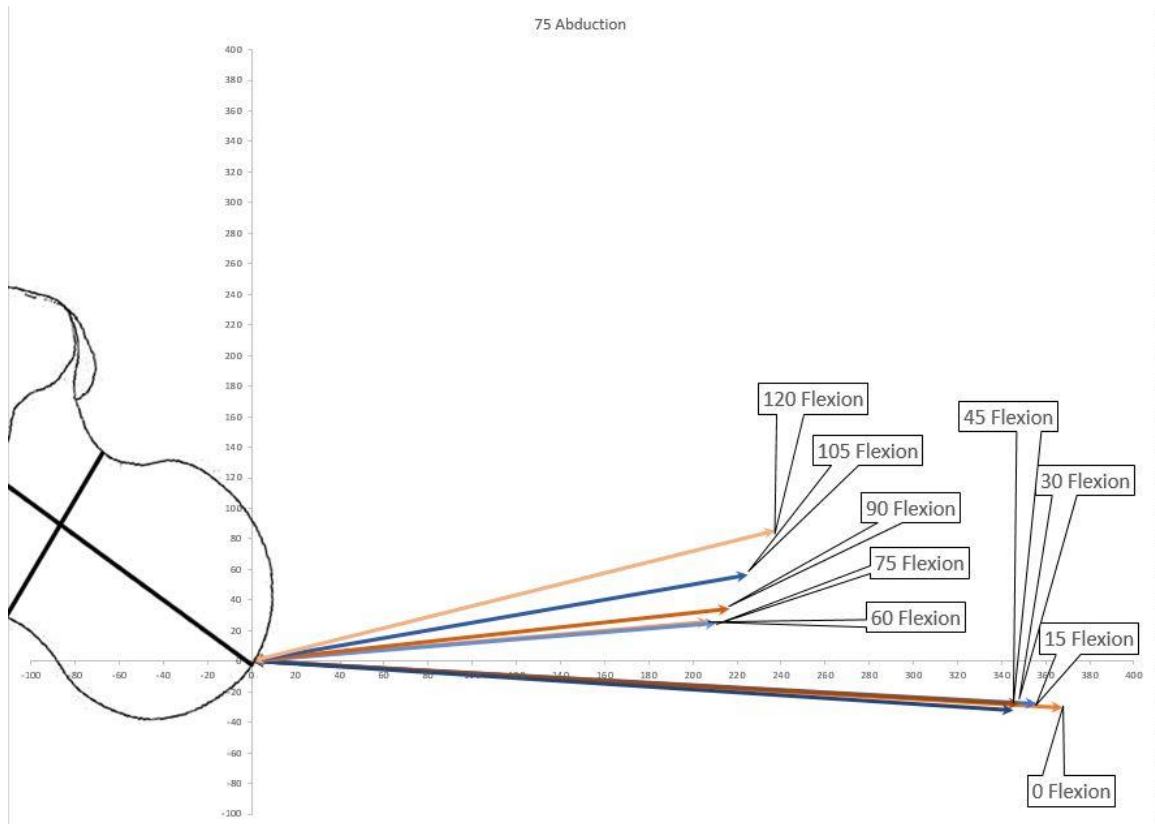


FIGURE 4.12: JRF magnitude and direction for 75 degrees of abduction with flexion varied on the axis

Chapter V

Discussion

This section discusses the results obtained from the joint kinematic analysis from the section above. The JRF vector output originates from the geometric center of the femur in the model. It is observed that for all cases increased abduction results in a greater joint reaction force magnitude. 75 Degrees of fixed abduction exhibit the greatest variance within the range of flexion, whereas 60 degrees of fixed abduction vary the least. It appears that 60 degrees of abduction involves the muscles in such a way that the baby can be put in any flexion position while abducted. Joint reaction forces also direct more in the anterior direction with increasing angles of flexion. At -15 degrees of abduction, the JRF direction moves towards the lateral direction, although force returns to pointing medially at higher degrees of flexion. An expected JRF magnitude of 240 was derived from [20] to compare to the results. This value is taken with respect to observation of an expected reaction force from a standing leg raise. It is reasonable to infer that a standing leg raise, where the hip is fixed at a flexed position and then supported, would provide similar reaction force magnitudes to hip positions done in the analysis. The value taken from [20] was 210 N, which is two times the weight of the infant model. This was then multiplied by an overestimation scale factor of 0.3 obtained from [21] that refers to the comparison between joint reactions obtained from OpenSim and *in vivo* reaction forces obtained via gait analysis experimentation. The value was compared to the dataset and the closest resultant magnitude was found to be the value from 60 degrees abduction and 120 degrees

flexion. The dataset was then normalized with respect to this value, which is similar to the value that Buschelberger stated to be beneficial for healthy hip development. A force vector angular deviation was also calculated with respect to this 60-120 value to identify the deviation of the resultant forces from this “healthy” value, as the vector found from the position coincides with the line passing through the geometric center of the acetabulum. The force directions are compared from the line that passes through the femur geometric center. The line was derived from the work done by Dostal and Andrews [22] and the joint reaction resultant vector was compared with this line to identify which positions produced forces that were most centrally located in the acetabulum. The diagrams above show that at 30-45 degrees of abduction produces centrally located forces for all flexions, suggesting that at any range of flexion in this abduction range, the muscles activate in such a way that settles the femoral head into the acetabulum.

Comparison with Existing Babywearing Positions

Conventional wisdom in regards to optimum babywearing practice asserts that high degrees of flexion, beyond 45 degrees of abduction, produce optimum JRF that coincide with healthy hip development. This is known as the M or spread-squat position. The results obtained show that the JRF does not deviate by much at 120 degrees of flexion beyond 15 degrees of abduction. The least deviation is in the range of 30-60 degrees of abduction. Buschelberger [2] has also hypothesized similarly that high flexion results in optimum contact forces, and his statement is also supported from the information above. The J shape position of

babywearing, which is a reduced amount of hip flexion compared to the M position, is advocated by manufacturers as another optimum position for healthy hip development. From inspection, the J shape usually involves hip flexions ranging between 90-110 degrees and reduced hip abductions below 60 degrees. The J shape provides good JRF magnitudes that are close to the magnitude found from the 60 abduction-120 flexion position; however, the increased deviation between abductions requires the baby to have their hips abducted more to achieve similar forces compared to the M shape. The JRF resultant vector direction also deviates from the M shape position with an almost 10% difference between the direction of the 60-120 position JRF vector, and the 45-105 position. The analysis of the Swaddling position, where the hips are negatively abducted, show that hip forces move far away from collinearity with the femur centerline. Negative abduction at all possible degrees of flexion has forces in the Z-component that direct laterally. This provides additional evidence that swaddling shallows the hip socket and increases the possibility of DDH to occur in the child.

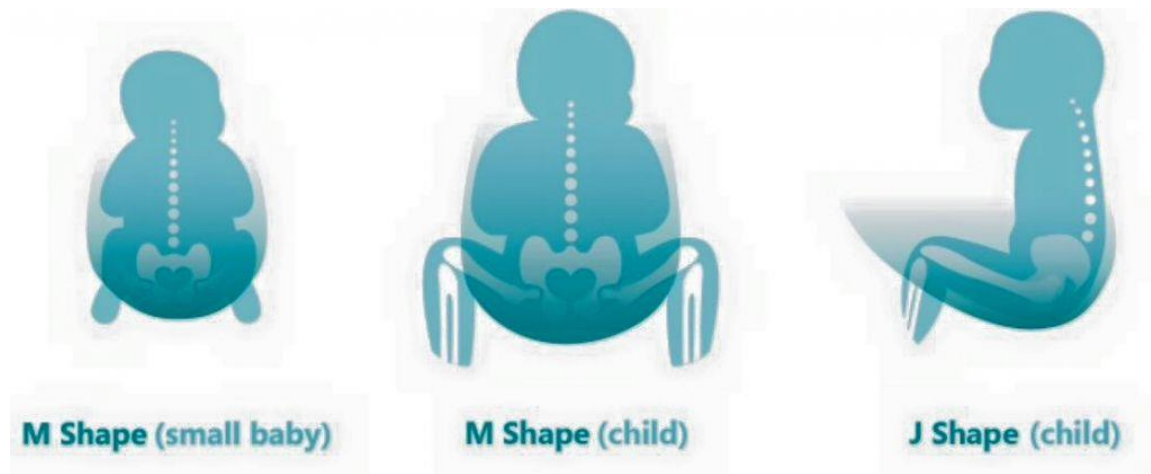


FIGURE 5.1: A visual of the babywearing styles most commonly recommended for healthy hip development, the M shape involves the baby pushed close to the chest, and the J shape involves the baby pushed close to the side of the carrier's body

TABLE 5.1: Normalized colormap indicating percent difference of the dataset with respect to the JRF magnitude value found from 60 abduction and 120 flexion, with green indicating closest to healthy

	0	15	30	45	60	75	90	105	120
-15	6.2%	-30.4%	-47.6%	-53.1%	-53.6%	-49.9%	-44.1%	-40.9%	-38.2%
0	5.7%	-32.7%	-50.9%	-57.1%	-58.4%	-53.1%	-42.9%	-31.8%	-22.1%
15	7.9%	-28.5%	-48.0%	-56.6%	-59.5%	-52.8%	-40.7%	-24.6%	-8.1%
30	13.2%	-20.2%	-39.8%	-49.2%	-55.8%	-49.3%	-36.7%	-19.1%	0.4%
45	23.8%	-4.2%	-22.0%	-31.1%	-47.2%	-41.8%	-30.9%	-15.5%	1.9%
60	43.2%	23.1%	9.5%	2.0%	-32.5%	-29.7%	-22.3%	-12.1%	
75	72.2%	63.2%	57.0%	53.6%	-12.6%	-11.6%	-8.7%	-3.3%	4.5%

TABLE 5.2: Normalized colormap indicating percent difference of the dataset with respect to the JRF vector direction found from 60 abduction and 120 flexion, with green indicating closest to healthy

	0	15	30	45	60	75	90	105	120
-15	55.1%	52.6%	49.2%	45.8%	40.7%	39.2%	39.1%	40.1%	41.5%
0	46.8%	43.4%	39.4%	35.9%	34.2%	33.0%	32.1%	32.3%	34.2%
15	39.0%	34.6%	29.8%	25.4%	26.6%	25.5%	25.3%	25.9%	27.2%
30	32.2%	27.4%	21.9%	16.1%	18.2%	17.2%	17.5%	18.5%	19.7%
45	27.0%	22.5%	17.1%	11.1%	10.7%	8.5%	8.7%	9.9%	11.0%
60	23.7%	20.5%	17.0%	13.6%	7.9%	4.3%	2.1%	0.8%	0.0%
75	22.6%	21.4%	20.3%	19.3%	12.4%	11.7%	11.9%	13.0%	13.9%

Chapter VI

Conclusion

A computational approach to determine reaction forces within a range of joint positions was successfully implemented. The existing human body model used in OpenSim was able to be scaled, tuned, and simplified in order to test the hypothesis and find the desired data. Joint reaction forces were successfully obtained for the full range of motion of the hip with a fixed external rotation. The results obtained were found to be in reason and provides new insight into the development of force within the range of motion of the infant hip. The work of Buschelberger was evaluated in light of the new findings and found to be consistent with his empirically-based hypothesis. The M position of babywearing, which involves subjecting the baby's hips to 60 degrees of abduction and 120 degrees of flexion is most conducive to healthy hip development, and companies such as Ergobaby should continue to develop products and devices with this position in mind.

Future Work

For the future work to improve this biomechanical study, the geometry of the model will be improved to make it more closely related to actual infant proportions. The impact of a change in femoral anteversion will also be investigated, and external rotation will also be varied to investigate its effect on reaction and muscle forces. The muscles would also be set at different activation levels to investigate the proportions of passive and active muscle tension in the reaction forces. Moreover, an optimization of the data set will be conducted to determine an optimal babywearing position. The modeling will also incorporate

finite-element analysis to determine the contact pressures within the hip socket, and also to determine the amount of coverage that the acetabulum provides while containing the femoral head in the different joint positions. Soft tissues such as cartilage and ligaments will also be incorporated in the overall analysis to increase simulation biofidelity.

Appendix A Bibliography

- [1] C. Nicolas Andry de Bois-Regard, *Orthopædia, or, The art of correcting and preventing deformities in children*, Classics of Medicine Library, 1980.
- [2] J. Büschelberger, "Studies on the peculiarities of the hip joint in infancy and their role in pathogenesis,," SLUB Dresden, 1961.
- [3] Orthoinfo, "Osteoarthritis," AAOS, 2014. [Online]. Available: <http://orthoinfo.aaos.org/topic.cfm?topic=a00227>.
- [4] S. M. M. E. L. S. K. M. C. T. P. H. S. Hosalkar, "Infantile DDH," 2010.
- [5] "Gray's Anatomy of the Human Body," Lea & Febiger, 1985.
- [6] S. R. W. R. L. L. S. L. D. E. M. Arnold, "A Model of the Lower Limb for Analysis of Human Movement," *Annals of Biomedical Engineering*, 2009.
- [7] W. H. R. H. S. F. Falkner, "Prenatal influences on postnatal growth: Overview and pointers for needed research," *European Journal of Clinical Nutrition*, pp. 48 Suppl 1:S15-22; discussion S22-4., February 1994.
- [8] E. Fettweis, "Carrying babies or toddlers in baby-carriers or shawls," *Orthopädische Praxis*, vol. 46, no. 2, pp. 93-98, 2010.
- [9] D. F. Huelke, "An Overview of Anatomical Considerations of Infants and Children in the Adult World of Automobile Safety Design," *Annual Process of the Association of Advancement of Automotive Medicine*, vol. 42, p. 93–113, 1998.
- [10] "Screening for developmental dysplasia of the hip: recommendation statement," *Pediatrics*, vol. 117, no. 3, 2006.
- [11] M. F. G. B. J. A. Lankester, "Adolescent hip dysplasia," vol. 18, no. 4, pp. 262-272, 2004.
- [12] M. D. J. Hornova, "Hip Joint Reaction Force Estimated using Opensim - Comparison to Measured Data," *ESB Congress*, 2013.
- [13] S. Kumar, *Biomechanics of Hip*, Narayana Medical College, 2013.
- [14] A. C. S. S. N. N. M. Giorgi, "Effects of normal and abnormal loading conditions on morphogenesis," *Journal of Biomechanics*, vol. 48, no. 12, p. 3390–3397, 2015.
- [15] E. S. R. T. Loder, "The Epidemiology and Demographics of Hip Dysplasia," *Journal of Orthopedics*, 2011.
- [16] A. Roper, "Hip Dysplasia in the African Bantu," *The Journal of Bone and Joint Surgery*, vol. 58, no. 2, pp. 155-158, 1976.
- [17] F. C. A. A. S. A. P. L. A. H. C. T. J. E. G. D. G. T. S. L. Delp, "OpenSim: Open-Source Software to Create and Analyze Dynamic Simulations of Movement," *IEEE Transactions on Biomedical Engineering*, vol. 54, no. 11, pp. 1940-1950, 2007.
- [18] J. M. L. C. W. J. H. S. M. Graham, "Back-carrying infants to prevent developmental hip dysplasia and its sequelae: is a new public health initiative needed?," *Journal of Pediatric Orthopedics*, vol. 35, no. 1, pp. 57-61, 2015.
- [19] D. R. C. S. Shefelbine, "Mechanobiological predictions of growth front morphology," vol. 22, no. 2, pp. 346-352, 2004.

- [20] R. Salter, "Etiology, Pathogenesis and Possible Prevention of Congenital Dislocation of the Hip," *The Canadian Medical Association Journal*, vol. 98, no. 20, pp. 933-945, 1968.
- [21] R. R. R. P. L. P. V. R. E. T. L. Wickiewicz, "Muscle Architecture of the Human Lower Limb," *Clinical Orthopedics and Related Research*, vol. 179, pp. 275-283, 1982.
- [22] J. G. A. W. F. Dostal, "A three-dimensional biomechanical model of hip musculature.," *Journal of Biomechanics*, vol. 14, no. 11, pp. 803-812, 1981.

Appendix B

Joint Reaction Force Table

Flexion (Degrees)	Abduction (Degrees)	X (N)	Y (N)	Z (N)	Magnitude (N)
0	-15	-134.236	-219.239	-33.091	259.191
15	-15	-44.398	-162.894	-18.380	169.834
30	-15	7.305	-127.463	-8.211	127.936
45	-15	41.407	-106.570	-1.352	114.339
60	-15	64.465	-92.110	13.116	113.190
75	-15	89.801	-81.065	17.281	122.206
90	-15	118.562	-64.792	18.110	136.319
105	-15	142.388	-16.236	15.562	144.153
120	-15	146.829	31.639	14.373	150.885
0	0	-134.589	-217.218	35.806	258.031
15	0	-42.976	-155.566	30.441	164.239
30	0	8.274	-115.903	28.935	119.746
45	0	39.609	-91.982	30.557	104.706
60	0	58.969	-76.278	31.457	101.415
75	0	85.548	-66.069	37.390	114.375
90	0	121.360	-48.552	48.222	139.323
105	0	155.714	-8.608	58.426	166.537
120	0	173.666	46.112	61.926	190.056
0	15	-139.927	-197.817	103.278	263.396
15	15	-51.018	-145.600	81.319	174.399
30	15	0.472	-106.774	68.351	126.778
45	15	31.647	-78.941	62.952	105.813
60	15	52.420	-65.453	52.152	98.751
75	15	80.968	-53.961	61.502	115.109
90	15	116.987	-34.977	77.667	144.712
105	15	155.550	0.161	98.320	184.018
120	15	182.219	53.755	118.942	224.144
0	30	-149.446	-162.145	166.304	276.192
15	30	-67.540	-125.033	133.305	194.846
30	30	-16.794	-93.766	111.793	146.873
45	30	16.794	-68.447	101.964	123.951
60	30	44.391	-58.165	79.295	107.895
75	30	71.039	-44.871	90.875	123.767
90	30	102.941	-26.511	112.083	154.474
105	30	137.400	3.778	141.766	197.461
120	30	163.648	49.170	175.453	244.913
0	45	-163.247	-114.055	227.164	302.095

15	45	-92.864	-94.256	192.784	233.823
30	45	-43.760	-74.134	169.836	190.408
45	45	-8.733	-54.294	158.783	168.036
60	45	29.686	-51.387	114.435	128.908
75	45	51.941	-37.498	126.724	141.996
90	45	75.111	-22.522	149.338	168.674
105	45	98.394	-2.308	181.085	206.103
120	45	116.725	25.227	218.239	248.775
0	60	-180.587	-52.902	294.583	349.556
15	60	-128.473	-47.382	267.476	300.489
30	60	-88.152	-38.069	249.349	267.199
45	60	-57.118	-25.170	240.898	248.853
60	60	3.623	-41.923	159.223	164.689
75	60	17.777	-30.708	167.832	171.542
90	60	29.192	-24.550	185.673	189.551
105	60	38.523	-21.525	209.882	214.471
120	60	47.214	-19.161	238.643	244.022
0	75	-200.488	30.321	367.933	420.106
15	75	-177.020	27.837	355.751	398.334
30	75	-157.434	28.129	348.248	383.215
45	75	-141.554	31.872	345.521	374.751
60	75	-41.078	-25.538	207.603	213.163
75	75	-36.867	-25.004	211.140	215.788
90	75	-38.265	-34.506	216.866	222.903
105	75	-41.649	-56.754	225.120	235.870
120	75	-39.189	-85.073	237.275	255.094

Appendix C

Example OpenSim Files

C. 1 Example Joint Kinematic Input File

```
Coordinates=
version=
1
nRows=50
1
nColumns=24
inDegrees=yes
endheader
```

	pelvis	pelvis	pelvis	pelvis	pelvis	pelvis	hip	hip	hip	ankle	ankle	mtp	hip	hip	ankle	ankle	mtp	lumb	lumb	
time	rotation	rotation	rotation	rotation	rotation	rotation	rotation	rotation	rotation	rotation	rotation	rotation	rotation	rotation	rotation	rotation	rotation	rotation	rotation	rotation
0.0	0	0	0	0	0	0	0	45	0	0	0	0	0	0	0	0	0	0	0	0
.02	0	0	0	0	0	0	0	45	0	0	0	0	0	0	0	0	0	0	0	0
.04	0	0	0	0	0	0	0	45	0	0	0	0	0	0	0	0	0	0	0	0
.06	0	0	0	0	0	0	0	45	0	0	0	0	0	0	0	0	0	0	0	0
.08	0	0	0	0	0	0	0	45	0	0	0	0	0	0	0	0	0	0	0	0
.1	0	0	0	0	0	0	0	45	0	0	0	0	0	0	0	0	0	0	0	0
.12	0	0	0	0	0	0	0	45	0	0	0	0	0	0	0	0	0	0	0	0
.14	0	0	0	0	0	0	0	45	0	0	0	0	0	0	0	0	0	0	0	0
.16	0	0	0	0	0	0	0	45	0	0	0	0	0	0	0	0	0	0	0	0
.18	0	0	0	0	0	0	0	45	0	0	0	0	0	0	0	0	0	0	0	0
.2	0	0	0	0	0	0	0	45	0	0	0	0	0	0	0	0	0	0	0	0
.22	0	0	0	0	0	0	0	45	0	0	0	0	0	0	0	0	0	0	0	0
.24	0	0	0	0	0	0	0	45	0	0	0	0	0	0	0	0	0	0	0	0

0																				
.2						1	-	-	-											
6	0	0	0	0	0	2	-	1	9	1		9	-	1	9	1				
0						0	45	0	0	0	0	0	10	0	0	0	0	0	0	0
.8						1	-	-	-											
8	0	0	0	0	0	0	45	0	0	0	0	9	-	1	9	1				
0						1	-	-	-											
.3						2	-	1	9	1		9	-	1	9	1				
3	0	0	0	0	0	0	45	0	0	0	0	0	10	0	0	0	0	0	0	0
0						1	-	-	-											
.3						2	-	1	9	1		9	-	1	9	1				
2	0	0	0	0	0	0	45	0	0	0	0	0	10	0	0	0	0	0	0	0
2						1	-	-	-											
.3						2	-	1	9	1		9	-	1	9	1				
4	0	0	0	0	0	0	45	0	0	0	0	0	10	0	0	0	0	0	0	0
0						1	-	-	-											
.3						2	-	1	9	1		9	-	1	9	1				
6	0	0	0	0	0	0	45	0	0	0	0	0	10	0	0	0	0	0	0	0
0						1	-	-	-											
.3						2	-	1	9	1		9	-	1	9	1				
8	0	0	0	0	0	0	45	0	0	0	0	0	10	0	0	0	0	0	0	0
0						1	-	-	-											
.4						2	-	1	9	1		9	-	1	9	1				
4	0	0	0	0	0	0	45	0	0	0	0	0	10	0	0	0	0	0	0	0
0						1	-	-	-											
.4						2	-	1	9	1		9	-	1	9	1				
2	0	0	0	0	0	0	45	0	0	0	0	0	10	0	0	0	0	0	0	0
0						1	-	-	-											
.4						2	-	1	9	1		9	-	1	9	1				
4	0	0	0	0	0	0	45	0	0	0	0	0	10	0	0	0	0	0	0	0
0						1	-	-	-											
.4						2	-	1	9	1		9	-	1	9	1				
6	0	0	0	0	0	0	45	0	0	0	0	0	10	0	0	0	0	0	0	0
0						1	-	-	-											
.5						2	-	1	9	1		9	-	1	9	1				
8	0	0	0	0	0	0	45	0	0	0	0	0	10	0	0	0	0	0	0	0
0						1	-	-	-											
.5						2	-	1	9	1		9	-	1	9	1				
0	0	0	0	0	0	0	45	0	0	0	0	0	10	0	0	0	0	0	0	0
.5						1	-	-	-											
4	0	0	0	0	0	0	45	0	0	0	0	0	10	0	0	0	0	0	0	0
0						1	-	-	-											
.5						2	-	1	9	1		9	-	1	9	1				
6	0	0	0	0	0	0	45	0	0	0	0	0	10	0	0	0	0	0	0	0
0						1	-	-	-											
.5						2	-	1	9	1		9	-	1	9	1				
8	0	0	0	0	0	0	45	0	0	0	0	0	10	0	0	0	0	0	0	0
0						1	-	-	-											
.6						2	-	1	9	1		9	-	1	9	1				
6	0	0	0	0	0	0	45	0	0	0	0	0	10	0	0	0	0	0	0	0
0						1	-	-	-											
.6						2	-	1	9	1		9	-	1	9	1				
2	0	0	0	0	0	0	45	0	0	0	0	0	10	0	0	0	0	0	0	0
0						1	-	-	-											
.6						2	-	1	9	1		9	-	1	9	1				
4	0	0	0	0	0	0	45	0	0	0	0	0	10	0	0	0	0	0	0	0
0						1	-	-	-											
.6						2	-	1	9	1		9	-	1	9	1				
6	0	0	0	0	0	0	45	0	0	0	0	0	10	0	0	0	0	0	0	0

C. 2 Example Joint Analysis Output File

Units are S.I. units (seconds,
meters, Newtons, ...)

endheader

time	hip_r_on_femur_r_in _ground_fx	hip_r_on_femur_r_in _ground_fy	hip_r_on_femur_r_in _ground_fz
0	1298.428758	787.8827214	1187.859825
0.02	1298.428758	787.8827214	1187.859825
0.04	1298.428758	787.8827214	1187.859825
0.06	1298.428758	787.8827214	1187.859825
0.08	1298.428758	787.8827214	1187.859825
0.1	1298.428758	787.8827214	1187.859825
0.12	1298.428758	787.8827214	1187.859825
0.14	1298.428758	787.8827214	1187.859825
0.16	1298.428758	787.8827214	1187.859825
0.18	1298.428758	787.8827214	1187.859825
0.2	1298.428758	787.8827214	1187.859825
0.22	1298.428758	787.8827214	1187.859825
0.24	1298.428758	787.8827214	1187.859825
0.26	1298.428758	787.8827214	1187.859825
0.28	1298.428758	787.8827214	1187.859825
0.3	1298.428758	787.8827214	1187.859825
0.32	1298.428758	787.8827214	1187.859825
0.34	1298.428758	787.8827214	1187.859825
0.36	1298.428758	787.8827214	1187.859825
0.38	1298.428758	787.8827214	1187.859825
0.4	1298.428758	787.8827214	1187.859825
0.42	1298.428758	787.8827214	1187.859825
0.44	1298.428758	787.8827214	1187.859825
0.46	1298.428758	787.8827214	1187.859825
0.48	1298.428758	787.8827214	1187.859825
0.5	1298.428758	787.8827214	1187.859825
0.52	1298.428758	787.8827214	1187.859825
0.54	1298.428758	787.8827214	1187.859825
0.56	1298.428758	787.8827214	1187.859825
0.58	1298.428758	787.8827214	1187.859825
0.6	1298.428758	787.8827214	1187.859825
0.62	1298.428758	787.8827214	1187.859825
0.64	1298.428758	787.8827214	1187.859825
0.66	1298.428758	787.8827214	1187.859825
0.68	1298.428758	787.8827214	1187.859825
0.7	1298.428758	787.8827214	1187.859825